Development of a Generalised Kinetic Model for the Combustion of Hydrocarbon Fuels

Author: Matthew Ryan Fry

Supervisor: Professor Klaus Möller

Thesis presented for the Degree of

Master of Science (Chemical Engineering)

in the Department of Chemical Engineering

University of Cape Town

May 2010

Acknowledgements

I wish to acknowledge and thank the following people:

- First and foremost my supervisor, Professor Klaus Möller, especially for all his effort in getting the final draft.
- Chris Woolard, Gareth Floweday, Marlan Perumal, Andy Yates and Carl Viljoen at the Sasol Advanced Fuel Labs for all their help and input.
- Sue Fry, my mom for her help with the final editing.
- The guys in the loft.

Development of a Generalised Kinetic Model for the Combustion of Hydrocarbon Fuels

Matthew Ryan Fry

20th May 2010

Abstract

The aim of this work is to find a generalised model for the combustion of hydrocarbons. Predicted temperature-time profiles can be obtained from detailed combustion kinetics, which can be used to derive a generalised model. If the generalised model can predict results from the detailed model it can be applied in computational fluid dynamics code where detailed kinetic mechanisms cannot.

A generalised kinetic model is proposed, adapting the Schreiber model (Schreiber et al., 1994) to accurately predict the combustion behaviour of hydrocarbon fuels. The combustion behaviour is described through the characteristics of the temperature-time profiles and the ignition delay diagram, which include two stage ignition and the negative temperature co-efficient region. The Schreiber model is specifically adapted to improve the description of the very low temperature rise before and between ignitions and the auto-catalytic temperature rises during ignition.

Using a Genetic Algorithm to optimise the prediction of the proposed model, the pre-exponent factor A_i and the activation energy Ea_i are the adjustable parameters which are optimised for each reaction in the model. These parameters have been optimised for three fuels: i-octane, n-heptane and methanol. The ignition delays of the pure fuels were accurately predicted. The temperature-time profiles in the instances of two stage ignition are relatively inaccurate. The temperature profiles are however an improvement on the temperature profiles predicted by the Schreiber model, particularly in terms of the slow temperature rise during the ignition delay and the sharp temperature rise during ignition.

The combustion of the binary blends of the three fuels have been predicted using model parameters which are found using the rate constants of each fuel, the blends composition and binary interaction rules. The binary interaction parameters were also optimised using a Genetic Algorithm. The binary interaction rules are based on the Peng-Robinson mixing rules. Overall the ignition delays of binary fuel blends were accurately predicted using binary interactions. However, when modelling the blends between methanol and n-heptane, where one fuel has extreme NTC behaviour and the other fuel has no NTC behaviour, the predictions were less accurate.

These binary interaction rules are then used to model ternary mixtures. It is shown that the combustion behaviour of ternary mixtures of the three fuels can be accurately predicted without any further regression or parameter fitting. The accuracy of the ternary prediction is dependent on the accuracy of the binary predictions.

Contents

List of Figures

List of Tables

Nomenclature

A Rate constant

a1, a2, a3, a4, a5 NASA coefficients for calculating heat capacity

a(T) Temperature dependent and compound specific parameter in Peng-Robinson equation

b Compound specific parameter in Peng-Robinson equation

C_3 and C_4 Adjustment parameters in the Schreiber model dependent on the fuels octane number

C Number of fuels in the blend

C_L Number of fuels in the blend with low temperature kinetics

Cor Square normalised correlation matrix

Cov Covariance matrix

Cp_i Heat capacity of compound i

Ea Activation energy

F Hydrocarbon fuel species

$[F_L]$ Concentration of fuel with low temperature kinetics

$[F_T]$ Total fuel concentration

H_i Enthalpy of compound i

$\triangle H_{rxn}$ Heat of reaction

I Hydrocarbon combustion intermediate species

J Jacobian

k_{ij} Interaction parameter between compound i and compound j

k Reaction rate

[M] Represents the total concentration of all the species

ne_{ij} Exponential binary interaction parameter for activation energy Ea

N_i Moles of compound i

n_{ij} Exponential binary interaction parameter for pre-exponent rate constant A

NOB Number of observations/Number of data points

p_0 Reference Pressure

P Hydrocarbon combustion product species

p^{vap} Vapour pressure

Q_loss Heat loss from system

R Universal gas constant

$SE_{parameter}$ Standard error of the parameter

$SE_{prediction}$ Standard error of the prediction

s Standard error

$T0_i$ Initial temperature i

$\tau_{ignition}$ Igntion delay (time)

$S(\theta)$ Objective function, sum of squares of the error

T Temperature

$\underline{V}$ Molar volume

we_{ij} Binary interaction parameter for activation energy Ea

w_{ij} Binary interaction parameter for pre-exponent rate constant A

W_s Work done on system

x_i Fraction of fuel i in the total fuel

X Hydrocarbon combustion intermediate species

y_i Fraction of fuel i in the total fuel with low temperature kinetics

Y_u	Observation/regression data point u
Y	Hydrocarbon combustion intermediate species
z_i	Third body efficiency for component i

Chapter 1

Introduction

1.1 Context

The efficiency of spark ignition engines is limited by the pre-ignition of the end gas within the engine chamber, a phenomenon known as "knock". Knock results in complications which will damage the engine (Warnatz et al., 2001). Engine efficiency can be improved by increasing the compression ratio, but this also increases knock potential. To mitigate this, the fuels need higher octane ratings and better burn properties. Concurrent to this are the tightening fuel specifications. Thus, there is incentive to develop accurate models for the combustion behaviour of complex fuels.

Conversely in homogeneous charge compression ignition (HCCI) engines, the ability to auto-ignite is a desirable attribute, as no spark is used to ignite the fuel (Andrae, 2008).

Before the spontaneous combustion of a fuel takes place there is an ignition delay time sometimes called an induction time. Within this period a very small temperature rise occurs while there is a slow build up of radicals and intermediates in the system until a critical concentration is reached for rapid ignition to take place. The ignition delay is one of the most important characteristics of a fuel. In a spark ignition engine the delay before the end gas auto-ignites needs to be long enough for complete combustion to take place in the engine chamber. The ignition delay before autoignition is an approximation of the time it takes for complete combustion, e.g., the reaction time to achieve 99% fuel conversion.

Taking into account all the possible radical reaction steps in the combustion of a typical fuel (e.g. i-octane) leads to kinetic models with around 2500 reaction steps and 2000 species (Curran et al., 2002). Despite increases in computing power, complete kinetic models for fuel blends are not practical when it comes to implementation. Therefore, simplification of the kinetic model is needed before they can be useful. Thus, the development of a robust, broadly applicable, simplified kinetic model is the first step to modelling the fuel's combustion. There are 2 approaches to obtaining reduced combustion kinetics, both are semi-empirical.

- Chemical: by reducing the detailed reaction mechanism using quasi-steady state or partial equilibrium, where assumptions are usually devised for certain conditions only (Warnatz et al., 2001).

- Physical: by considering the key physical chain-thermal behaviour and developing a set of reaction steps that represent the autoignition but are not necessarily actual chemical species. For example, the physical model's intermediates will represent a large group of intermediates in the detailed kinetic model.

When reducing a large mechanism, the form of the elementary steps and, thus, the elementary kinetic expressions are retained. These reduced mechanisms cannot be extrapolated to other conditions (e.g. temperature and pressure) without the introduction of non-elementary kinetics, which would defeat the objective of the reduction process. Physical models combine mechanistic combustion chemistry with experimental observations to obtain reaction steps and species that can describe the observed trends through the parameterisation of non-elementary kinetic expressions over a broad range of conditions. It is important in the model that chemical and thermal feedback interactions are described from first principles.

It is also important that the model describes the reaction paths in the low temperature range ($<$1000 K) as well as the high temperature range. The low temperature oxidation is important in obtaining the ignition delay, while the high temperature is important for describing flame propagation (Schreiber et al., 1994). The model also needs to use thermal and chemical feedback for the prediction of ignition in order to assist in the prediction of multi-stage ignition and the negative temperature dependence of ignition delay shown by some hydrocarbons (Schreiber et al., 1994).

1.2 Scope

The aim of this work is to find a generalised model for the combustion of hydrocarbons. Most models, detailed and generalised, are based on and validated using ignition delay diagrams. These models could potentially be far more accurate if they were based on temperature-time profiles, but the data is difficult to obtain experimentally. Predicted temperature-time profiles can be obtained from detailed combustion kinetics, which can be used to derive a generalised model. If the generalised model can predict results from the detailed model it can be applied in computational fluid dynamics code (CFD).

A generalised model is proposed which is designed to capture the very low temperature rise before and between ignitions and the auto-catalytic temperature rises during ignition. The proposed model should have the ability to describe the features seen in the autoignition of firstly n-heptane and then applied to other hydrocarbons. The model should be complete in terms of describing systems with varying temperatures, compositions and pressures.

The properties of the proposed model will be derived directly from the more comprehensive kinetic models simulated in CHEMKIN, a powerful software system for solving complex chemical kinetics problems. The detailed chemical kinetic mechanisms were obtained from Curran et al. (1998) for n-heptane and Curran et al. (2002) for i-octane. The proposed model is based on these detailed kinetic models for two reasons. First it is difficult to obtain meaningful experimental data, as in most cases the experiments are limited to low pressures and then only cover a small range of conditions and secondly, because it avoids any ambiguous boundary conditions (Schreiber et al., 1994). It also gives access to temperature and concentration time profiles over the complete region.

Once a robust model has been developed, linear and quadratic mixing rules will be developed to model the oxidation of binary mixtures using binary interaction rules, as is done in the mixture rules for the Peng-Robinson equations of state. New rate constants for the fuel blend will be found using the rate constants of each fuel, the blend's composition and binary interaction functions. These binary interaction rules will then be used to model ternary mixtures. Therefore the blend will have its own unique set of constants which can be used in a combustion simulation. Importantly the blend will have the same number of constants and reactions as a pure fuel.

In this work, the proposed model will be parameterised for three fuels: i-octane, n-heptane and methanol. Their binary interaction parameters will be obtained from binary blends and they will be used to predict ternary mixtures of the three fuels.

A generalised model that can model a highly detailed mechanism would be a step toward modelling experimental data. If the generalised model can accurately reproduce results of the detailed model in a CHEMKIN simulation it will be a useful tool in CFD calculations. If the concept of using binary interactions to accurately model a ternary mixture works there is potential for modelling

other ternary blends and more complex mixtures that are considered suitable as gasoline or diesel surrogates.

Chapter 2

Literature Review

2.1 Relevance of Autoignition

2.1.1 Engine Knock

Knock is a problem in the common spark-ignited engine, i.e. the Otto engine. The overall efficiency of the engine is increased by increasing compression ratio of the engine but this simultaneously increases the likelihood of knock.

In an engine cylinder the last remaining unburnt gas behind the spark-ignited flame front is called the end-gas. The piston compression together with the advancing flame front, heat and compress the end gas. If the pressure and temperature of the end gas is low enough, the end gas will not autoignite and the flame front will engulf the end gas. Alternatively, the end gas reactions might progress too rapidly, and the end gas will ignite before the flame front arrives, setting up pressure waves. The delay before ignition takes place is very temperature sensitive and local hot spots are able to initiate autoignition. This phenomenon is known as knock and it creates pressure peaks which can damage the piston and engine. Increasing the compression ratio, calculated from the cylinder dimensions, increases the likelihood of knock.

Fuels differ in their tendency to produce knock and this tendency is defined by their octane number. A fuel's octane number is relative to n-heptane and i-octane. N-heptane with a high tendency to knock is defined as having an octane number of 0, whilst i-octane, with a low tendency to knock, is defined as having an octane number of 100.

The onset of autoignition is governed by chemical kinetics and the temperature and pressure of the system (Warnatz et al., 2001).

2.2 Understanding Autoignition

2.2.1 Autoignition Phenomenon

A combustion model should be able to describe three types of behaviour that are seen in combustion:

1. High temperature kinetics, in which fuels are decomposed into small hydrocarbons followed by oxidation (Muller et al., 1992). The heat release in these reactions must yield the adiabatic flame temperatures. The high temperature oxidation is important for describing flame propagation (Schreiber et al., 1994).

2. Low temperature kinetics, in which the reversible temperature is dependent on two stage O_2 addition and chain branching is accounted for. Chemical feedback dominates in this region and thermal effects are minimal. However, slight heating should stop the chain branching, thus producing the Negative Temperature Coefficient (NTC) behaviour (Warnatz et al., 2001). The low temperature oxidation is important in predicting the ignition delay (Schreiber et al., 1994).

3. The benchmark of most combustion models, detailed or generalised is the ability to accurately model the NTC region. Ignition delay generally decreases with an increase in starting temperature, a relationship which is reversed in the NTC region. Ignition delay is proportional to the overall combustion system's rate constant. It can be seen in figure 2.1 that at low and high temperatures the ignition delay depends exponentially on the reciprocal temperature, which exhibits Arrhenius temperature dependence (Warnatz et al., 2001).

$$\tau_{ignition} = Ae^{\frac{B}{T}} \tag{2.1}$$

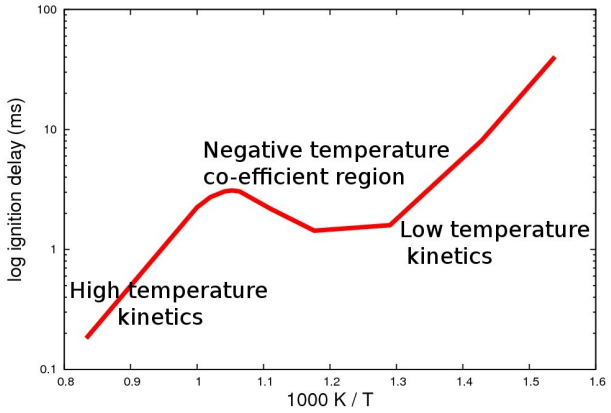

Figure 2.1: Ignition delay for the combustion of a stoichiometric mixture of n-heptane-air under adiabatic conditions, simulated in CHEMKIN using detailed kinetics (Curran et al., 1998).

This complex dependence seen in the NTC region in figure 2.1, is a result of the kinetic interactions associated with low temperature reversible oxidation (Griffiths, 1995). The shorter ignition delays at higher temperature are caused by multi-stage ignitions, where there are rises in temperature prior to the final ignition. This phenomenon is clearly illustrated in figure 2.2 where the 2 stage ignition of n-heptane is illustrated. The first ignition in the 2 stage ignition is referred to as the 'cool' flame. Looking at the curves as they increase in the initial temperature, it can be seen how the ignition delays decrease at low temperatures, then increase at the intermediate temperatures (950K) and then decrease again.

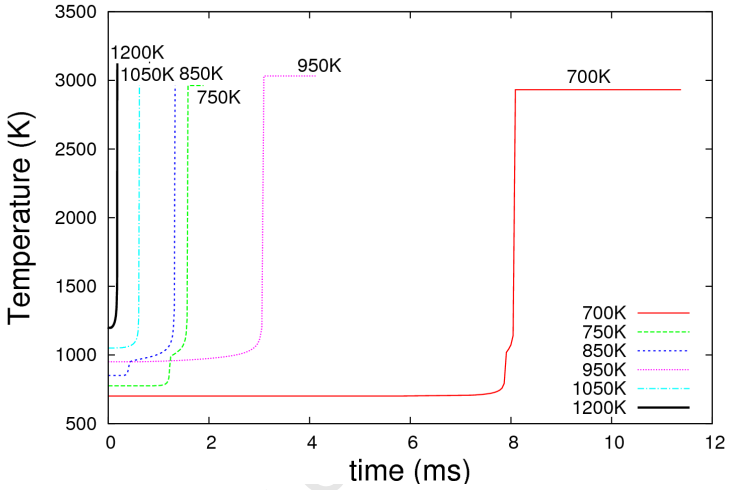

Figure 2.2: Temperature-time profiles for the combustion of stoichiometric mixture of n-heptane-air under adiabatic conditions and at various starting temperatures, simulated in CHEMKIN using detailed kinetics (Curran et al., 1998).

2.2.2 Combustion Chemistry

The development of comprehensive detailed reaction mechanisms for the oxidation of hydrocarbons has shown that their high temperature ignition (T>1100K) can be described by 9 elementary classes of reactions, while the low and intermediate temperature ignition (T<1100K) is far more complex and a further 16 classes of elementary reactions are required (Yates and Viljoen, 2008). The key elements of hydrocarbon combustion are summarised by Chevalier et al. (1992) and Warnatz et al. (2001). The primary chain branching steps above 1100 K are:

$$H\bullet + O_2 \Rightarrow O\bullet + OH\bullet \tag{2.2}$$

Between 900 and 1100 K :

$$OH_2\bullet + RH \Rightarrow H_2O_2 + R\bullet \tag{2.3}$$

$$H_2O_2 + M \Rightarrow OH\bullet + OH\bullet + R\bullet \tag{2.4}$$

R is a alkyl radical, Q is a olefin and M represents the third body interactions. Below 900K (the important region for the NTC), one possible route is:

First O_2 addition	$$R\bullet + O_2 \Longleftrightarrow RO_2\bullet$$	(2.5)
External abstraction	$$RO_2\bullet + RH \Rightarrow ROOH + R\bullet$$	(2.6)
Chain branching	$$ROOH \Rightarrow RH\bullet + OH\bullet$$	(2.7)
Internal abstraction	$$RO_2\bullet \Rightarrow Q\bullet OOH$$	(2.8)
Chain propagation	$$Q\bullet OOH \Rightarrow QO + OH\bullet$$	(2.9)

Internal abstraction is seen to dominate and the only route to excessive chain branching is through the addition of another O_2 to QOOH:

Second O_2 addition	$$Q\bullet OOH + O_2 \Rightarrow O\bullet OQOOH$$	(2.10)
External abstraction	$$O\bullet OQOOH + RH \Rightarrow HOOQOOH + R\bullet$$	(2.11)
Chain branching	$$HOOQOOH \Rightarrow HOOQO\bullet + OH\bullet$$	(2.12)
Chain propagation	$$HOOQO\bullet \Rightarrow OQO + OH\bullet$$	(2.13)
Internal abstraction	$$O\bullet OQOOH \Rightarrow HOOQ'O\bullet OOH$$	(2.14)
Chain propagation	$$HOOQ'O\bullet OOH \Rightarrow HOOQ'O + OH\bullet$$	(2.15)
Chain branching	$$HOOQ'OO\bullet \Rightarrow OQ'O\bullet + OH\bullet$$	(2.16)

The low temperature steps ($<$ 900K) are dependent on the chemical nature of the reactant, the mobility of the H atom and the stability of the hydroperoxy radical. These reactions supply the required chemical feedback that is necessary to produce the NTC behaviour.

Chain branching is the formation of radicals (or reactive intermediates) from the stable reactants. The chain branching increases the pool of radicals exponentially, leading to rapid combustion and the explosion of the reaction. Chain propagation is the reaction of radicals with stable reactants. Chain termination is where the reactive species are removed by forming stable species. Termination can either occur homogeneously in the gas phase with third body collisions or heterogeneously with the combustion chamber wall.

2.2.3 'Cool' Flame Chemistry

It is accepted that the 'cool' flame phenomenon is dependent on an underlying chemical equilibrium reaction, which is the combination of alkyl radicals $R\bullet$ with oxygen, as in reaction 2.5.

The equilibrium constant for the reaction is strongly temperature dependent. The forward reaction is favoured at lower temperatures, changing to favour the reverse reaction as the temperature increases (Yates and Viljoen, 2008). So the reaction is 'switched off' with an increase in temperature which is why the reaction is so important in describing the 2 stage ignition.

2.3 Modelling Fuel Oxidation

Zheng et al. (2004) put chemical kinetic models into five categories, which are discussed in this section and summarised in table 2.1. A sixth category of models not covered by Zheng et al. (2004) are the single-stage Arrhenius-based models which have historically been the first attempts to describe autoignition. More recently Yates and Viljoen (2008) have developed a formulation with two Arrhenius reactions, which is also discussed in this section.

Table 2.1: Summary of the five categories of chemical kinetic models (Zheng et al., 2004)

Category	Description	Species	Reactions
Detailed models	The latest "comprehensive" reaction list	100's	1000's
Lumped models	Uses a lumped description for larger species	100's	1000's
Reduced models	A subset of the detailed model	10's	100's
Skeletal models	Employs class chemistry and lumping concepts	10's	10's
Global / Generalised models	Utilises global reactions to minimise reaction set	<10	<10

2.3.1 Detailed Models

Detailed models attempt to be as comprehensive as possible and therefore include all the important elementary reactions and individual species using the best available rate parameters and thermo-chemical data (Zheng et al., 2004). This is not an easy exercise. Firstly, it is difficult to identify the important reactions and species, both of which number in the 1000's. Secondly, the rate constants for each reaction have to be found experimentally and if that is not possible, by computational approximation (Lu and Law, 2009). A detailed mechanism is judged to be comprehensive based on its ability to provide predictions across a range of conditions: temperature, pressure and composition. It also needs to include low, intermediate and high temperature chemistry (Lu and Law, 2009).

Examples of detailed models are Curran et al. (1998) for n-heptane and Curran et al. (2002) for i-octane. For an excellent review of detailed gas-phase kinetic models developed to simulate the low-temperature oxidation and autoignition of gasoline and diesel fuel components and some of their mixtures, refer to Battin-Leclerc (2008).

Kolaitis and Founti (2009) compared detailed, semi-detailed and reduced mechanisms for n-heptane. The kinetic mechanisms were used in CHEMKIN to simulate reactions in two different reactors

using perfectly stirred reactor/jet stirred reactor (JSR) assumptions and plug flow reactor (PFR) assumptions. The mechanisms were a range of sizes and, as anticipated, increasing the number of species and reactions improves the prediction quality. However, compared to experimental data even the detailed mechanisms still had significant discrepancies. The poor performance of the reduced and semi-detailed mechanisms (shown in table 2.2), show that model developers tend to focus on the medium-to-high temperature and pressure conditions found in internal combustion engines (Kolaitis and Founti, 2009).

Table 2.2: Comparison of kinetic mechanisms' general performance (Kolaitis and Founti, 2009)

No. of Species	Target Application	Intermediate Pressure JSR			Low Pressure JSR	PFR
		T<640 K	NTC	T>750 K		
22	HCCI combustion	-	-	+	+	+++
27	Prediction of ignition	++	+	++	+	+
41	High-T oxidation	-	-	++	-	-
44	High-T oxidation	++	++	+++	++	+
57	Reduced from 561 species	+++	+++	++	++	+++
561	Detailed mechanism	+++	+++	+++	++	+
645	Detailed mechanism	+++	+++	+++	+++	-

Legend: +++, quantitative agreement; ++, qualitative agreement; +, significant discrepancies; –, no chemical activity.

Detailed models are often only for single hydrocarbons and are validated for a very limited range of conditions Zheng et al. (2004). Therefore, the mechanisms cannot be used for fuel blends or gasoline surrogates. Mehl et al. (2009) have revised earlier kinetic mechanisms for n-heptane, i-octane and toluene and merged them so that they can be used to model complex gasoline surrogates. The decomposition rates and the thermal properties of several radicals were revised, which significantly influenced the general reactivity of i-octane and makes it possible for greater accuracy over a wide range of operating conditions (Mehl et al., 2009).

Using this merged mechanism they analysed the behaviour of important surrogate components, in particular n-heptane, i-octane, butane, 1-hexene and toluene. The mechanism is used for predictions of various fuels and blends, which are compared with experimental data collected in a rapid compression machine, shock tube and jet stirred reactors. Figure 2.3 is a typical example of the correlation obtained by Mehl et al. (2009) between their results and the experimental data.

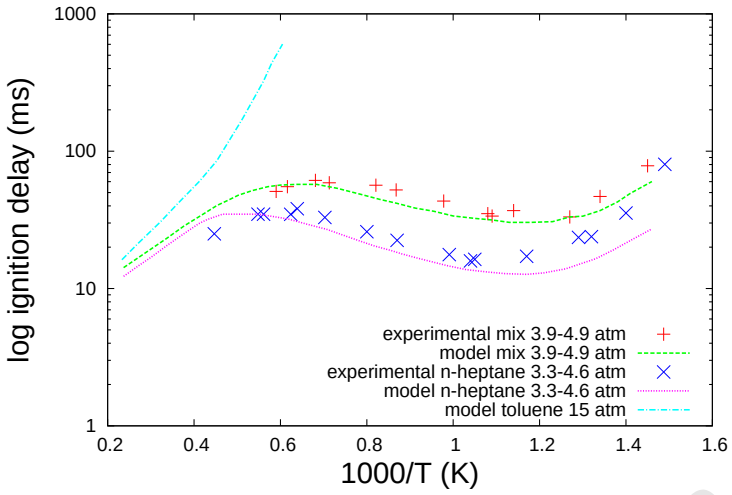

Figure 2.3: Comparison of experimental and simulated ignition delay times of the toluene/n-heptane mixture and its pure components (Mehl et al., 2009)

2.3.2 Lumped and Reduced Models

In order to make the mechanisms less computationally expensive, these model types are an attempt use the detailed model to derive smaller models which remain accurate. The lumped model is derived by grouping correlated species so that the number of variables described by differential equations is reduced. Since lumping the species may result in duplicate reactions, the number of reactions can be reduced as well (Lu and Law, 2009). Examples of lumped models are Violi et al. (2002) and Agosta et al. (2004).

A reduced model contains only the most critical elements from the detailed mechanism and they are reduced using quasi-steady state analysis and partial equilibrium assumptions (Warnatz et al., 2001). Examples of reduced models are Frenklach and Wang (1991) and Lu et al. (2003).

Both reduced and lumped mechanisms are usually only developed to predict combustion over a small range of temperature and pressure. Unsatisfactory performance is obtained outside the range of temperature and pressure for which the kinetic models were developed (Warnatz et al., 2001).

The reduction of detailed models has the following shortcomings:

- By definition the reduced model will only contain elementary reactions, so it cannot describe non-elementary behaviour.
- The number of reactions are still too many for realistic use in CFD.
- Carbon and other elemental balances are not always conserved.

Future models will need to overcome these limitations.

2.3.3 Skeletal Models

Skeletal models consist of a composite of kinetic steps including elementary, generic or global reactions. The rate parameters and thermochemistry represent 'classes of reactions'. The models are effective at describing low and intermediate temperature chemistry and Zheng et al. (2004) have used skeletal models to simulate pre-ignition behaviour, ignition time and combustion rate in homogeneous charge compression ignition (HCCI) engines. A skeletal model with 69 reactions and 45 species was used, which is still too large to maintain acceptable computational time when combined with CFD code.

2.3.4 Global/Generalised Models

Generalised models describe the chemistry in terms of a few principal reactants and products. The goal is to minimise the mechanism to make it conducive to CFD calculations. At the same time the number of variables is reduced, making empirical regression simpler. Generally, these models have had more success predicting high temperature oxidation (Zheng et al., 2004). Efforts to include intermediate and low temperature oxidation have been made by Muller et al. (1992) with their 4-reaction model and by Schreiber et al. (1994) with their 5-reaction model. The 4-reaction model relied only on thermal feedback for its prediction, which resulted in a qualitative failure to capture the NTC behaviour. In the Schreiber model they introduced chemical auto-catalysis and extended the applicability of their model to fuels beyond n-heptane (Schreiber et al., 1994). The Schreiber model is an adaptation of a 9 reaction mechanism from Griffiths (1993) which in turn used ideas from Cox and Cole (1985) and it is described in more detail in section 2.5. More recently Zheng et al. (2004) adapted the Schreiber model to develop the Zheng model, a global model more suited for the prediction of HCCI behaviour.

Global mechanisms are often only useful over a limited range of temperatures and pressures and although the approach is useful in solving certain systems it does not provide any chemical understanding of the systems (Turns, 2000).

2.3.5 Arrhenius Equation based Models

Single-stage Arrhenius-based models are commonly used but they lack detail regarding the 'cool' flame phenomenon (Yates et al., 2010). Yates and Viljoen (2008) developed a more sophisticated Arrhenius empirical model which has the capability to describe both the 'cool' flame and the overall autoignition response to pressure, temperature and air–fuel ratio. The model is not based on any specific chemical reactions, but is rather setup with a generic formulation specifically to obtain the 'hot' and 'cool' flame ignition delays.

The model simplifies the overall ignition delay into four basic steps: (1) a pre-cool-flame delay at constant temperature, (2) an instantaneous 'cool' flame temperature increase (which could be zero), (3) a further delay at constant temperature, and (4) the final exothermic 'hot' flame auto-ignition (Yates et al., 2010). Two Arrhenius reaction formulations are used in the model, one for the 'hot' and one for the 'cool' flame ignitions. The two Arrhenius terms are in the form:

$$\tau = Ap^n e^{\frac{B}{T}}, \tag{2.17}$$

where τ represents the ignition delay for a stoichiometric constant-volume mixture initially at pressure p and temperature T. The coefficients A, n and B are constants (Yates and Viljoen, 2008). The two Arrhenius formulations are coupled through the thermal feedback given by the 'cool' flame ignition to the 'hot' flame ignition. The two Arrhenius formulations had no chemical interaction so there was no chemical feedback from the 'cool' flame, which is required when modelling two stage combustion. Yates and Viljoen (2008) included chemical feedback by using a simple multiplying factor 'X' in the post 'cool' flame ignition delay calculation.

Despite the Arrhenius model's success it is not usable in CFD work because it does not provide the reaction rates and heat release needed to carry out the simulations.

2.4 Surrogate Fuels

Gasoline fuels are very complex due to the continuous spectrum of hydrocarbon components (Andrae, 2008). Therefore, simplification is needed to help provide insight and understanding into the combustion of gasoline. This can be done by using a surrogate gasoline fuel with a limited number of compounds and a standard composition as close as possible to practical fuels. The problem is that the fuels blend differently. The gasoline surrogate may have the same octane number and ignition delay as gasoline, but the reaction path taken to achieve the same ignition delay will not necessarily be the same.

2.4.1 RON and MON

Empirical measures like octane number are used to categorise a fuel with respect to their resistance in terms of ignition behaviour. The octane numbers of a fuel and its surrogate are used to justify the suitability of the surrogate. There are two common standards for obtaining a fuel's octane number, the research octane number (RON) and the motor octane number (MON). The RON and MON scales are both based on the primary reference fuels (PRF) where i-octane (RON = MON = 100) and n-heptane (RON = MON = 0). RON is higher than MON for non-PRFs and both

standards of any non-PRFs only describe autoignition behaviour at the respective test conditions. The numbers are not always helpful in characterising fuels for modern internal combustion engines (Andrae, 2008).

Viljoen (2009) constructed a simple linear model to estimate the %NTC associated with a compound based on its molecular structure. The %NTC is then used to predict the RON and MON for the compounds.

2.4.2 Gasoline Surrogates

Single and double component fuels have been used as surrogates for gasoline for many years and are extremely useful in some engines and operating conditions. However, they do not reproduce gasoline behaviour over the wide range of conditions, for example the operating conditions of a HCCI engine (Andrae, 2008).

The components of European gasoline can be divided into six families, each having a carbon number ranging from 4 to 10. They are linear alkanes (n-paraffins), branched alkanes (i-paraffins), ethers, cyclic alkanes (napthenes), alkenes (olefins) and aromatic compounds (Battin-Leclerc, 2008). Gauthier et al. (2004) state that the following are the major components present in gasoline: cyclo-pentane, toluene, i-pentane, meta-xylene, 3-methylhexane, n-heptane, 2-methylhexane, ethylbenzene, n-pentane and i-octane.

Pitz et al. (2007) suggest that the three components in a gasoline surrogate should be n-heptane, i-octane and toluene. n-Heptane represents the linear alkanes, i-octane the branched/cyclo alkanes, and toluene the aromatics (Machrafi and Cavadias, 2008). More specifically:

- n-heptane represents n-heptane and n-pentane;
- i-octane represents cyclo-pentane, i-pentane, 3-methylhexane, 2-methylhexane, and i-octane; and
- toluene represents toluene, meta-xylene, and ethylbenzene.

Other fuels that need to be considered in a gasoline surrogate are ethanol and diisobutylene. Ethanol is the main biofuel component in practical fuels and diisobutylene is a common olefin (Fikri et al., 2008).

The use of a single member of a hydrocarbon class to represent the autoignition characteristics of the whole class will not always be accurate. An example is the olefin, 1-hexene, which displays significant NTC behaviour, while internal olefins such as 2-hexene and 3-hexene have little or no NTC character (Viljoen et al., 2005). This is because the degree of NTC behaviour can be related to the availability of a chain of at least 3 carbons next to one another in the structure of the molecule

(Tanaka et al., 2003). This is because the more carbons there are in a chain, the more secondary hydrogens there are in the molecule. The reason secondary hydrogens increase NTC behaviour is explained by Viljoen et al. (2005): "If these carbons contain secondary hydrogens (i.e. the two hydrogens bonded to a secondary carbon atom), then the low temperature oxidation pathways can easily proceed through many possible low-strain ring structures (from 5 to 8-membered rings during internal H abstraction). The higher the number of secondary hydrogens, the more pronounced the NTC character becomes."

2.4.3 Validation of Surrogates

Machrafi and Cavadias (2008) used an HCCI engine to experimentally compare the performance of gasoline 95, a PRF95 (5 vol% n-heptane and 95 vol% i-octane) and the gasoline surrogate (11 vol% n-heptane, 59 vol% i-octane, and 30 vol% toluene), all with an octane number of 95. For both the pressure and the heat release (shown in figure 2.4), the gasoline surrogate and gasoline 95 compare quite satisfactorily but the PRF95 shows significant discrepancies. Therefore the surrogate is validated but the octane number is shown to be an unsuitable indicator for the appropriateness of a surrogate fuel. Figure 2.4 reiterates the fact that fuels with the same octane number do not always have the same ignition behaviour or delay.

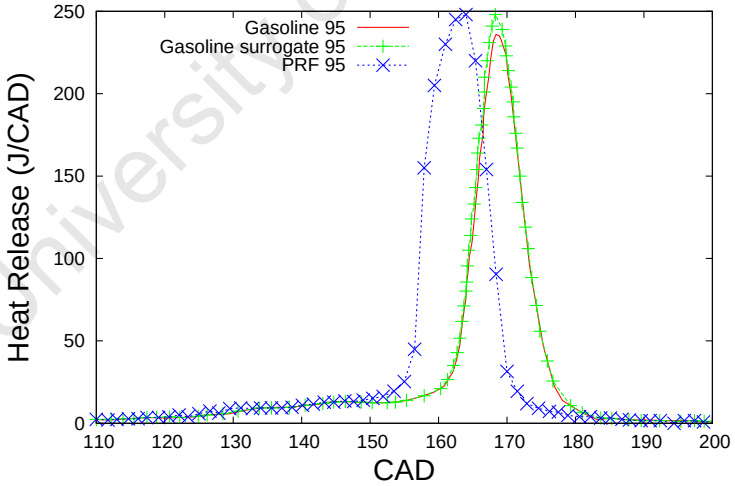

Figure 2.4: Comparison of the heat release profiles using three fuels with an octane number of 95, at an inlet temperature of 70°C, a compression ratio of 13.5, and an equivalence ratio of 0.462 The 'cool' flame delay is defined as the crank angle degrees' (CAD) interval from the bottom dead centre (BDC) to the final ignition(Machrafi and Cavadias, 2008) .

Fikri et al. (2008) used shock-tube experiments to determine ignition times for various stoichiometric mixtures of two multi-component model fuels in air. The fuel blends were n-heptane(18%), i-octane(62%) and ethanol (20%) by liquid volume and n-heptane(20%), toluene (45%), i-octane

(25%) and diisobutylene (10%) by liquid volume. These fuels have octane numbers comparable to a standard European gasoline of 95 RON and 85 MON and both surrogates produced ignition delay diagrams similar to that of the gasoline.

2.5 The Schreiber Model

2.5.1 Structure of the model

Using the physical approach, Schreiber et al. (1994) proposed a 5 reaction model which, building on the model of Muller et al. (1992), accurately predicts alkane ignition delays.

Table 2.3: Schreiber five step reduced scheme for n-heptane

Reaction no.	Reaction	Reaction Rates
1	$F \rightarrow X$	$R_1 = k_1[F](\frac{p}{p_0})^{0.5}$
2	$X + 11O_2 \rightarrow P$	$R_2 = k_2[X][O_2][M]$
3+	$F + 2O_2 \rightarrow I$	$R_{3+} = k_{3+}[F][O_2][M](\frac{p}{p_0})^{-2.2}C_3$
3-	$I \rightarrow F + 2O_2$	$R_{3-} = k_{3-}[I](\frac{p}{p_0})^{-3.5}$
4	$I \rightarrow 2Y$	$R_4 = k_4[I]C_4$
5	$Y + 0.5F + 10O_2 \rightarrow P$	$R_5 = k_5[O_2][Y]$

$[M] = \frac{p}{RT}$ represents the total concentration of all the species. C_3 and C_4 are the adjustment parameters depending on the fuel characteristics, namely the octane number. $\left(\frac{p}{p_0}\right)$ represents the variation of reaction rates with pressure.

The rate coefficients have a temperature dependence described by the Arrhenius law,

$$k_i = A_i * e^{\frac{Ea_i}{RT}}, \tag{2.18}$$

where A_i and Ea_i are the adjustable parameters in the model.

2.5.2 Features of the Schreiber Model

The reduced model emulates the oxidation of n-heptane (Warnatz et al., 2001). Reactions 1 and 2 describe the high temperature oxidation. The oxidation of F (n-heptane) yields the intermediates represented by X ($C_2H_4 + CH_2 + CH_3 + H$). Reactions 3, 4 and 5 describe the low temperature oxidation. The oxidation of F (n-heptane) yields the free radicals and intermediates I and Y ($OC_7H_{13}O_2H + H_2O$). The final products are assumed to be $7CO_2 + 8H_2O$. Although the reaction rates are non-elementary, they bear a close resemblance to the chemical equations and are

stoichiometrically consistent. In Reaction 3 both the first and the second O_2 additions are subsumed. The reversible second O_2 oxidation is where the mechanism for obtaining 2 stage ignition is represented in this model (Warnatz et al., 2001). The temperature sensitive equilibrium Reaction 3 is responsible for the switching the branching Reaction 4 on or off. At low temperatures the addition of O_2 is favoured and thus Reaction 4 proceeds, leading to low temperature combustion with slow heating. A subtle temperature increase due to the low temperature combustion results in the reverse of Reaction 3 slowly being favoured. This slows the low temperature branching Reaction 4 and reduces the production rate of intermediates and the temperature rise. The production of the high temperature radicals proceeds slowly, thus there is a another delay before the final ignition.

The Schreiber model can be extended to 'non-NTC' fuels. Toluene and ethanol can be shown from the detailed kinetic model to be 'non-NTC' fuels. Therefore the simplified chemical kinetic scheme can be taken as the higher temperature kinetic scheme for i-octane (Reactions 1 and 2).

Schreiber's model can also be used to model PRF blends. Here the constants C_3 and C_4 can be scaled according to the octane number of the blend.

2.5.3 Model Validation

The Schreiber model was parameterised using a detailed kinetic model of hydrocarbon oxidation (Schreiber et al., 1994). The model was again validated for the ignition delay diagrams of single component fuels, using CHEMKIN 3.7 to simulate combustion with detailed kinetic mechanisms (Viljoen et al., 2005). In the validation process, the parameters were reparameterised using data from CHEMKIN simulations of detailed mechanisms. The detailed mechanisms were obtained from Curran et al. (1998) for n-heptane and Curran et al. (2002) for i-octane.

Like many models, simple or detailed, the Schreiber model is based on correctly modelling the ignition delay diagram. This means the model was parametrised to only predict the time delay before the ignition of the fuel takes place, not the temperature profile over that time. Combustion models have been validated using experimentally obtained ignition delay diagrams instead of temperature-time profiles, because the temperature-time profiles are very difficult to obtain experimentally.

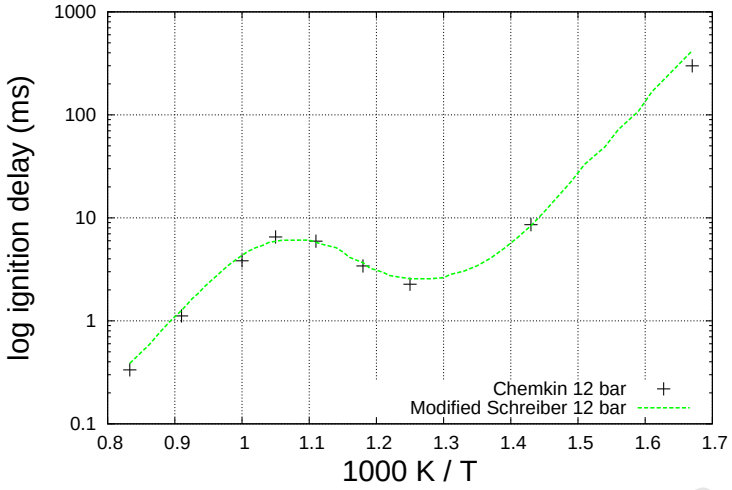

Figure 2.5: Ignition delay for n-heptane at 12 bar, Schreiber model compared to literature data (After having been adjusted to the same pressure) (Viljoen et al., 2005).

The parameter estimation was based on a constant volume adiabatic bomb and a constant heat capacity (Schreiber et al., 1994). The heat capacity of the system was assumed to be roughly equal to that of N_2 which is the main component in the system (roughly 78% in a stoichiometric mixture of fuel and air). The reaction enthalpies were adapted to ensure the adiabatic flame temperature was reached at the end of combustion. In accord with Hess's Law the overall enthalpies of combustion are equal, irrespective of the path taken from fuel to product.

The Schreiber model does have its shortcomings. It does not accurately model the heat release before the 'cool' flame for the temperature-time profile (Viljoen, 2009). Detailed kinetic simulations predict an almost constant temperature whereas the Schreiber model predicts a gradual temperature rise right from the start in the constant volume adiabatic system.

2.5.4 Modelling mixtures using the Schreiber model

The Schreiber model can be used as a prediction tool for PRFs (i-octane and heptane) and their blends using octane number which works well, but it has been validated for blends of i-octane and n-heptane only. Viljoen et al., 2005 proposed modelling all blends by enlarging the mechanism to include the different species, which were assumed to produce the same intermediates. However, the object of a reduced mechanism is then defeated as a 300 component fuel will produce thousands of reactions.

2.6 Third Body Efficiency

Termolecular recombination reactions are an important class of reactions within post-flame chemistry, responsible for a bulk of the heat release (Ashman and Haynes, 1998). The general form of a termolecular reaction is given by Turns (2000):

$$A + B + M \rightarrow C + M \tag{2.19}$$

Examples of important termolecular reactions in combustion are (Turns, 2000):

$$H + H + M \rightarrow H_2 + M \tag{2.20}$$

$$H + OH + M \rightarrow H_2O + M \tag{2.21}$$

In these reactions reactants collide with a 'third body' M, which transfers some of the translational kinetic energy from the 'third body' to the reactant (Turns, 2000). This increases the internal vibrational and rotational energies of the reactant (Turns, 2000), catalysing the reaction. Molecules have different 'third body efficiencies'. In the reaction $H + O_2 + M \rightarrow H_2O + M$, the third-body efficiency for H_2O is reported to be up to 15 times that of N_2 (Ashman and Haynes, 1998). For the same reaction, Ashman and Haynes (1998), determined third-body efficiencies for H_2O, CO_2 and Argon relative to N_2 to be 10.6, 2.4, and 0.56, respectively.

2.7 Parameter Estimation

2.7.1 Gradient based methods

Most gradient based methods for estimating reaction rate constants in chemical reactions systems use the same basic idea. Starting with an initial guess for the parameters the following two steps are repeated until desired accuracy is reached or the system diverges:

1. Integrate the system of differential equations and evaluate the objective function
2. Adjust the parameter values in order to minimise objective function.

The methods vary in the way the parameters are updated in step 2. Various rules may be employed for choosing the search direction and a fixed, variable or random step size can be used (Elliott et al., 2004).

According to Elliott et al. (2004) there are three main difficulties faced in a reaction rate parameter estimation problem, namely:

1. The objective function $f(x)$ is not available in a closed form; only its values at given points can be calculated.
2. The derivatives of function $f(x)$ are not available.
3. The number of kinetic parameters is very large.

When these gradient based methods fail rigorous models have to be simplified or reduced, meaning that solutions could be lost (Hughes, 2009). As an alternative, stochastic methods can be used. They have no problem with discontinuities but are heavy on function evaluations and therefore computationally expensive. Genetic Algorithms (GA) provide a non-gradient based method to minimise the objective function.

2.7.2 GREG

A good example of a gradient based method is the method used by the FORTRAN package, GREG. Parameters are estimated by minimising a statistical objective function $S(\theta)$, usually using least squares minimisation. The minimisation is done using a modified Newton method. $S(\theta)$ is approximated across the feasible region using a quadratic function $\tilde{S}(\theta)$. The point of minimum $\tilde{S}(\theta)$ is found using a quadratic programming subroutine. The point is then tested with the true objective function. The steps are repeated till the error is below tolerance or the maximum iterations are reached.

2.7.3 Genetic Algorithm (GA)

A GA takes a random group of potential solutions and, by applying genetic operators to the group, the best solution is found.

A general description of a GA (Davis, 1996):

1. Initialise a population of sets of parameter values
2. Evaluate each parameter set in the population
3. Select the best parameter set from the population to act as 'parents' in the new population
4. Create new parameter sets by combining the 'parents' to generate new parameter sets. Mutation also occurs to to ensure that random parameter sets enter the population to explore new regions of potential solutions.

5. Delete members of the population to make space for the new parameter sets
6. Evaluate the new parameter sets and insert them into the population
7. Repeat steps 3 to 5 until the maximum number of generations are reached.

Generations refer to the number of times new parameter sets are developed and evaluated.

GA are very robust because they differ from most methods in the following ways (Elliott et al., 2004).

- They search from a population of points, not from a single point. No function gradients are used.
- They use payoff information based upon an objective function, rather than derivatives or other auxiliary knowledge.
- They use probabilistic transition rules, not deterministic rules, to guide their search.
- They are able to depart from local optima and find the the global optimum.

Elliott et al. (2005) used a real coded GA that optimised reaction rate coefficients against ignition delays and species concentration-time profiles.

2.8 Peng-Robinson Mixing Rules

This study aims to use a generalised kinetic model for a pure fuel and adapt it to be usable for mixtures by combining the rate constants of the pure fuels in the mixture using proposed mixing rules. Similarly, the Peng-Robinson equation of state which is used to calculate the vapour pressure for pure species can also be used to calculate the vapour pressure for mixtures. The Peng-Robinson equation is one of the newer and more accurate equations of state available. Sandler (2006) presents the Peng-Robinson equation as the most accurate equation of state to date.

The Peng-Robinson equation of state for a pure gas, where a and b are parameters that are unique to the pure gas (Sandler, 2006):

$$p^{vap} = \frac{RT}{\underline{V} - b} - \frac{a}{\underline{V}(\underline{V} + b) + b(\underline{V} - b)} \tag{2.22}$$

When the gas is a mixture, the vapour pressure (p^{vap}) can be found using the same equation of state except new values for the parameters a and b are needed for the mixture.

$$p_{mix}^{vap} = \frac{RT}{\underline{V} - b_{mix}} - \frac{a_{mix}}{\underline{V}(\underline{V} + b_{mix}) + b_{mix}(\underline{V} - b_{mix})} \tag{2.23}$$

a_{mix} and b_{mix} have to be obtained for the gaseous mixture. b_{mix} is obtained using a linear combination. The Peng-Robinson mixing rule for b_{mix} is (Sandler, 2006):

$$b_{mix} = \sum_{i=1}^{C} y_i b_i \tag{2.24}$$

a_{mix} is obtained using a quadratic combination, which uses the binary interaction parameters (k_{ij}). The Peng-Robinson mixing rule for a_{mix} is (Sandler, 2006):

$$a_{mix} = \sum_{i=1}^{C} \sum_{j=1}^{C} y_i y_j \sqrt{a_i a_j}(1 - k_{ij}) \tag{2.25}$$

The interaction parameters, k_{ij}, are evaluated empirically from data for gaseous binary mixtures. The k_{ij} values are unique for each binary mixture. They represent a correction to the vapour pressure of a gaseous mixture between component i and component j.

The need for similar mixing rules in this study make the Peng-Robinson binary mixing rules a suitable starting point for creating the binary mixing rules for finding the rate constants of fuel mixtures to be used in the proposed generalised kinetic model. Linear combinations like equation 2.24 will be the starting point. Should they be insufficient, quadratic combinations similar to equation 2.25 will be used and binary interaction parameters like k_{ij} will have to obtained empirically.

Chapter 3

Project Objectives

The objectives of this study are as follows:

1. To obtain a simple generalised kinetic model for the combustion of n-heptane which can describe all the features of the temperature-time profiles and the ignition delay diagrams.

2. To extend the generalised kinetic model further to be able to model the combustion of n-heptane at different system conditions, specifically at different starting temperatures and pressures. This will be achieved by adding adjustable constants to the model.

3. The generalised kinetic model needs to be able to be re-parameterised to model the combustion of other hydrocarbons. This will be done for i-octane and methanol.

4. To develop mixing rules in order to model the combustion of binary hydrocarbon blends and to parameterise the mixing rules to describe the combustion behaviour of binary blends between i-octane, methanol and n-heptane.

5. To use the binary interactions to describe the combustion behaviour of the ternary blends involving: i-octane, n-heptane and methanol. This will validate the concept of using binary interactions to model multi-component fuels.

Chapter 4

Theory

4.1 Reactor Model

4.1.1 Assumptions

The data obtained from the CHEMKIN simulations are based on certain assumptions. For consistency the same assumptions have to made in the reactor model. Those assumptions are that the reactor is:

- a closed combustion bomb,
- adiabatic and spatially homogeneous,
- filled with a stoichiometric mixture of fuel and air.

The gas inside the combustion bomb is assumed to obey the ideal gas law.

4.1.2 Mass Balance

The concentration profiles are obtained from the mass balance.

$$\frac{dN_i}{dt} = r_i V \tag{4.1}$$

4.1.3 Energy Balance

The temperature profile is obtained from the energy balance. The system is assumed to be an adiabatic batch reactor where there is no heat loss, therefore $Q_{loss} = 0$.

$$Q_{loss} - W_s = \frac{\partial E_{sys}}{\partial t} \tag{4.2}$$

There is no work done on this system so $W_s = 0$.

$$0 = \frac{\partial E_{sys}}{\partial t} \tag{4.3}$$

Then using $E_{sys} = N_i H_i - Vp$ and the fact that the volume is constant the following equation is obtained:

$$\frac{\partial E_{sys}}{\partial t} = \sum N_i \frac{\partial H_i}{\partial t} + \sum H_i \frac{\partial N_i}{\partial t} - V\frac{\partial p}{\partial t} = 0 \tag{4.4}$$

Within equation (4.4) the following is known:

$$\frac{\partial H_i}{\partial t} = Cp_i \frac{\partial T}{\partial t} \tag{4.5}$$

Then substituting equation (4.5) and the mass balance, equation (4.1) into equation (4.4) the following is obtained:

$$0 = \frac{\partial T}{\partial t} \sum N_i Cp_i + \sum H_{rxn,i} r_i V - V\frac{\partial p}{\partial t} \tag{4.6}$$

Using the ideal gas law we get the following:

$$pV = \sum N_i RT \tag{4.7}$$

Differentiating with respect to time, with volume constant:

$$V\frac{\partial p}{\partial t} = RT \sum \frac{\partial N_i}{\partial t} + \sum N_i R \frac{\partial T}{\partial t} \tag{4.8}$$

Equation 4.8, when substituted into equation (4.6) the final energy balance is obtained:

$$0 = \frac{\partial T}{\partial t} \sum N_i Cp_i + \sum H_{rxn,i} r_i V - RT \sum \frac{\partial N_i}{\partial t} - \sum N_i R \frac{\partial T}{\partial t} \tag{4.9}$$

Rearranging, the final energy balance is obtained:

$$\frac{\partial T}{\partial t} = \frac{-\sum H_{rxn,i} r_i V + RT \sum \frac{\partial N_i}{\partial t}}{\sum N_i (Cp_i - R)} \tag{4.10}$$

4.2 Thermo-chemical Properties

4.2.1 Temperature Dependent Heat Capacity

The Schreiber model (Schreiber et al., 1994) assumes a constant heat capacity for the system, independent of composition and temperature. For the proposed model a temperature dependent global heat capacity for the model is derived using the NASA development with the NASA coefficients from Thergas (Muller et al., 1995) and based on composition of the system.

Thergas is a computer program permitting the automatic computation of the heat of formation, entropy and the heat capacity of molecules and free radicals in the gas phase. These calculations use the methods proposed by Benson (1976), which include bond and group additivity with ring, cis, ortho, gauche, symmetry and optical isomer corrections, analysis of differences between a free radical and its parent molecule. The only input to the program is the molecular formula of species. The output of Thergas can be chosen to be in the form of NASA coefficients. The coefficients are used in the following equation:

$$Cp(T) = a1 + a2 * T + a3 * T^2 + a4 * T^3 + a5 * T^4 \tag{4.11}$$

The intermediates represented in a generalised kinetic model are not specified exactly, so the heat capacities are calculated based on the known fuel, air, products and their mole fractions. The intermediates present are assumed to have similar heat capacities to the equivalent oxygen and fuel used to produce them.

4.2.2 Pressure Dependent Reaction Rates

The proposed model has a pressure dependence which is similar in form to the Schreiber model. An example is given below where α is the parameter adjusted to account for pressure change.

$$R = k * [A][B](\frac{p}{p_0})^{\alpha}, \tag{4.12}$$

where P_0 is the reference pressure.

4.2.3 Third Body Efficiency

$$M = z_{N_2}[N_2] + z_{O_2}[O_2] + z_{CO_2}[CO_2] + z_{H_2O}[H_2O] \tag{4.13}$$

Using equation 4.13 for the contribution of the third body efficiency, the following values were found to give the best results where $z_{N_2} = z_{O_2} = 0.1$ and $z_{CO_2} = z_{H_2O} = 6.0$

The literature on third body efficiency implies that the z values vary significantly between reactions and there are no final validated values.

4.3 Generalised Kinetic Models

4.3.1 The Schreiber Model

The Schreiber model (Schreiber et al., 1994) is described in detail in the literature review. The Schreiber model is shown below for comparison with model B and model C. The Schreiber model for n-heptane is based on the basic oxidation reaction:

$$C_7H_{16} + 11O_2 \Rightarrow 7CO_2 + 8H_2O \tag{4.14}$$

Table 4.1: Model A, Schreiber five step reduced scheme for n-heptane

High Temperature Kinetics			
Reaction no.	Reaction	Reaction Rates	$\triangle H_{rxn}$(kJ/mol)
A1	$F \rightarrow X$	$R_1 = k_1[F](\frac{p}{p_0})^{0.5}$	709.9
A2	$X + 11O_2 \rightarrow P$	$R_2 = k_2[X][O_2][M]$	-4709.9
Low Temperature Kinetics			
Reaction no.	Reaction	Reaction Rates	$\triangle H_{rxn}$(kJ/mol)
A3+	$F + 2O_2 \rightarrow I$	$R_{3+} = k_{3+}[F][O_2][M](\frac{p}{p_0})^{-2.2}C3$	-53.9
A3-	$I \rightarrow F + 2O_2$	$R_{3-} = k_{3-}[I](\frac{p}{p_0})^{-3.5}$	53.9
A4	$I \rightarrow 2Y$	$R_4 = k_4[I]C4$	-60.0
A5	$Y + 0.5F + 10O_2 \rightarrow P$	$R_5 = k_5[O_2][Y]$	-3913.1

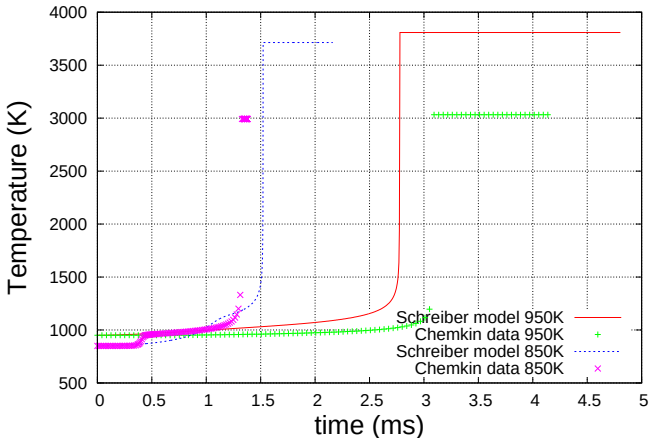

Figure 4.1: Temperature profiles comparing the Schreiber model to CHEMKIN simulation data (using detailed kinetics from Curran et al. (1998)) for the combustion of n-Heptane in a combustion bomb at 20 bar two initial temperatures, 850K and 950K.

When comparing the temperature-time profiles obtained from CHEMKIN with those obtained by the Schreiber model in figure 4.1, the Schreiber model fails to capture the slow temperature rise in both the first and second ignition delays as well as the sharp temperature rise in the first ignition. This is the same criticism of the model made by Viljoen (2009).

The Schreiber model is used as the basis for the proposed model. The adjustments to the Schreiber model are mainly in the low temperature oxidation kinetics. In order to describe the multi-stage ignition the model has to contain a 'switching off' mechanism where the source of free radicals to the system is 'switched off' by the increase in temperature. In the Schreiber model, Reaction A3 is the reversible reaction which is'switched off' by the increase in temperature.

However, by virtue of the Schreiber mechanism, Reaction A3+ is at its fastest initially. It then slows down gradually as it approaches the 'switching off' temperature. In order for Reaction A3+ not to shut down prematurely and stop 'cool' flame oxidation happening at all, Reaction A4 needs to be fast in converting I to Y. An early increase in Y means an early start for Reaction A5, which means that the temperature rises faster than it should during the ignition delay. The fast Reaction A4 combined with the slowing down of Reaction A3+ mean that the Schreiber models prediction of the heat release is unsatisfactory. There needs to be a very gradual acceleration of Reaction A5, which the Schreiber model cannot achieve.

The following kinetic models were developed to improve the temperature-time profiles, improve the ignition delay prediction and provide a more accurate interpretation of the auto-catalysis.

4.3.2 Proposed Model B

Table 4.2: Proposed Model B, five step generalised kinetic model for n-heptane

High Temperature Kinetics			
Reaction no.	Reaction	Reaction Rates	$\triangle H_{rxn}$(kJ/mol)
B1	$F \rightarrow X$	$R_1 = k_1 M[F](\frac{p}{p_0})^a$	709.9
B2	$X + 11O_2 \rightarrow P$	$R_2 = k_2[X][O_2]$	-4709.9
Low Temperature Kinetics			
Reaction no.	Reaction	Reaction Rates	$\triangle H_{rxn}$(kJ/mol)
B3	$F + 2O_2 \rightarrow I$	$R_3 = k_3[F][O_2](\frac{p}{p_0})^b$	20.0
B4+	$I + F + 2O_2 \rightarrow 2I$	$R_{4+} = k_{4+}[I][F][O_2](\frac{p}{p_0})^c$	20.0
B4-	$2I \rightarrow I + F + 2O_2$	$R_{4-} = k_{4-}[I]$	-20.0
B5	$I + 9O_2 \rightarrow P$	$R_5 = k_5[O_2][I]^2$	4000.0

In Model B, the very slow initial temperature rise is captured by Reaction B3. Eventually Reaction B4, which is auto-catalytic, gets going and provides the intermediates to ignite Reaction B5. Reaction B5 provides the heat which 'switches off' Reaction B4. The interaction between Reactions B4 and B5 is critical in obtaining the gradual temperature rise before ignition as well as the steep temperature rise during ignition.

As in the Schreiber model the high temperature chemistry is easily summarised by the two global reactions (Muller et al., 1992).

4.3.3 Proposed Model C

Model B when compared with the Schreiber model, reduces the number of species from six to five. However when dealing with binary fuel blends between fuels with and without low temperature kinetics it becomes necessary to distinguish between the two categories of fuels within the mechanism. Model B is adjusted to generate Model C accordingly.

In the final proposed mechanism, model C, $[F_T]$ is the total fuel concentration and $[F_L]$ is the concentration of fuel with low temperature kinetics. This implies previous knowledge of the fuel's ignition behaviour. This knowledge will be clear from the ignition delay data which will in any case be needed when parameterising the model for the different fuels.

$$F_T = F_L + fuel\ with\ only\ high\ temperature\ kinetics$$

F_T is recalculated at each time step in the integration to ensure that the same fuel is not burnt twice: in the low temperature kinetics and in the high temperature kinetics.

Table 4.3: Proposed Model C, five step generalised kinetic model for n-heptane

High Temperature Kinetics			
Reaction no.	Reaction	Reaction Rates	$\triangle H_{rxn}$(kJ/mol)
C1	$F_T \rightarrow X$	$R_1 = k_1 M[F_T](\frac{p}{p_0})^a$	709.9
C2	$X + 11O_2 \rightarrow P$	$R_2 = k_2[X][O_2]$	-4709.9
Low Temperature Kinetics			
Reaction no.	Reaction	Reaction Rates	$\triangle H_{rxn}$(kJ/mol)
C3	$F_L + 2O_2 \rightarrow I$	$R_3 = k_3[F_L][O_2](\frac{p}{p_0})^b$	20.0
C4+	$I + F_L + 2O_2 \rightarrow 2I$	$R_{4+} = k_{4+}[I][F_L][O_2](\frac{p}{p_0})^c$	20.0
C4-	$2I \rightarrow I + F_L + 2O_2$	$R_{4-} = k_{4-}[I]$	-20.0
C5	$I + 9O_2 \rightarrow P$	$R_5 = k_5[O_2][I]^2$	4000.0

The high temperature kinetics remain the same as in the Schreiber model where the oxidation of F (n-heptane) yields the intermediates X ($C_2H_4 + CH_2 + CH_3 + H$). Reactions C3, C4 and C5 describe the low temperature oxidation. The oxidation of F (n-heptane) yields the free radicals and intermediate I ($OC_7H_{13}O_2H + H_2O$). The final products are assumed to be $7CO_2 + 8H_2O$. In Reaction C4 both the first and the second O_2 additions are subsumed.

4.3.4 Generalised Kinetic Model for i-Octane and Methanol

The five step generalised kinetic model for n-heptane is adapted for i-octane based on the basic oxidation reaction of i-octane:

$$C_8H_{18} + 12.5O_2 \Rightarrow 8CO_2 + 9H_2O \tag{4.15}$$

Table 4.4: Model D, proposed model C adapted for i-octane

High Temperature Kinetics			
Reaction no.	Reaction	Reaction Rates	$\triangle H_{rxn}$(kJ/mol)
D1	$F_T \rightarrow X$	$R_1 = k_1 M[F_T](\frac{p}{p_0})^a$	709.9
D2	$X + 12.5O_2 \rightarrow P$	$R_2 = k_2[X][O_2]$	-5209.9
Low Temperature Kinetics			
Reaction no.	Reaction	Reaction Rates	$\triangle H_{rxn}$(kJ/mol)
D3	$F_L + 2O_2 \rightarrow I$	$R_3 = k_3[F_L][O_2](\frac{p}{p_0})^b$	20.0
D4+	$I + F_L + 2O_2 \rightarrow 2I$	$R_{4+} = k_{4+}[I][F_L][O_2](\frac{p}{p_0})^c$	20.0
D4-	$2I \rightarrow I + F_L + 2O_2$	$R_{4-} = k_{4-}[I]$	-20.0
D5	$I + 10.5O_2 \rightarrow P$	$R_5 = k_5[O_2][I]^2$	4500.0

The five step generalised kinetic model for n-heptane is adapted for methanol based on the basic

oxidation reaction of methanol:

$$CH_4O + 1.5O_2 \Rightarrow CO_2 + 2H_2O \tag{4.16}$$

Methanol was chosen because it represents a high octane component that is present in the detailed reaction mechanisms for i-octane and n-heptane. Methanol does not exhibit a 'cool' flame and it is therefore likely to produce blending behaviour of multi-component gasoline and typical future synthetic fuels (Yates and Viljoen, 2008). Methanol has no NTC behaviour because the methanol molecule has only one carbon and at least a three carbon chain is generally needed for a molecule to display NTC behaviour (Tanaka et al., 2003). Therefore methanol does not need low temperature kinetics in order to predict its combustion behaviour.

Table 4.5: Model E, proposed model C adapted for methanol

High Temperature Kinetics			
Reaction no.	Reaction	Reaction Rates	$\triangle H_{rxn}$(kJ/mol)
E1	$F_T \rightarrow X$	$R_1 = k_1 M[F_T](\frac{p}{p_0})^a$	-60.0
E2	$X + 1.5O_2 \rightarrow P$	$R_2 = k_2[X][O_2]$	560.0

4.3.5 Finding the Heat of Reactions

The heats of reactions are estimated from candidate reactions which are likely to take place. For Reaction C1 in the combustion of n-Heptane, where the reaction can be assumed to be $C_7H_{16} \rightarrow 3C_2H_4 + CH_3 + H$ the heat of reaction is:

$$\triangle H_{rxn} = [3(52.3) + 143.51 + 218.0] - (-187.78) = 706.19 kJ/mol$$

For Reaction C2 in the combustion of n-Heptane, where the reaction can be assumed to be $3C_2H_4 + CH_3 + H + 11O_2 \rightarrow 7CO_2 + 8H_2O$ the heat of reaction is:

$$\triangle H_{rxn} = [8(-241.8) + 7(-393.51)] - [3(52.3) + 143.51 + 218.0 + 11(0.0)] = 5207.4 kJ/mol$$

The heats of reactions for fuel mixtures is covered in section 4.4.

4.3.6 Thermodynamic Inconsistencies

Equilibrium constants can be calculated from the second law of thermodynamics (Levenspiel, 1999). Therefore the equilibrium constant for reversible reaction A3 in the Schreiber model can be expressed in terms of partial pressures as follows:

$$Ke = \frac{\prod\limits_{products}\left(\frac{f_i}{f_i^o}\right)}{\prod\limits_{reactants}\left(\frac{f_i}{f_i^o}\right)} = \frac{\prod\limits_{products} p_i^v}{\prod\limits_{reactants} p_i^v} = \frac{p_I}{p_F p_{O_2}^2} \tag{4.17}$$

Ideal gas conditions can be assumed because the operating temperatures are very high, $p = CRT$. Therefore the equilibrium constant can be expressed in terms of concentration:

$$Ke = \frac{C_I}{C_F C_{O_2}^2} . \frac{1}{R^2 T^2} \tag{4.18}$$

or alternatively:

$$Ke = \frac{[I]}{[F][O_2]^2} . \frac{1}{R^2 T^2} \tag{4.19}$$

Equilibrium for reaction A3 in the Schreiber model is obtained using the rate expressions R_{3+} and R_{3-}.

$$\frac{k_{3-}}{k_{3+}} = \frac{[I](\frac{p}{p_0})^{-3.5}}{[F][O_2][M](\frac{p}{p_0})^{-2.2}} \tag{4.20}$$

$Ke \neq \frac{k_{3-}}{k_{3+}}$ therefore the rate expressions in the Schreiber model are thermodynamically inconsistent. Similarly the equilibrium constant for reversible reaction C4 in the proposed model C can be expressed in terms of concentration using equation 4.18. Equilibrium is obtained for reaction C4 in model C using the rate expressions R_{4+} and R_{4-}.

$$\frac{k_{4-}}{k_{4+}} = \frac{1}{[F][O_2](\frac{p}{p_0})^{-1.4}} \tag{4.21}$$

$Ke \neq \frac{k_{4-}}{k_{4+}}$ therefore the rate expressions in model C are also thermodynamically inconsistent. The inconsistencies are caused by the corrections to the rate expressions needed to describe the ignition behaviour of n-heptane. Expressions such as these are common in reduced models in order that they capture the true dynamics of combustion. They have been used successfully in literature over the past 30 years.

4.4 Developing Mixing Rules

4.4.1 Basic Concepts for Multi-feed First Order Reactions

The basic method of combining rate constants and activation energies was investigated using a simple scenario where two different reactants form two products. The two reactions, their rate constants and their heats of reaction are combined to obtain one overall reaction with one reaction rate and one heat of reaction.

$$B_1 \rightarrow P_1$$

$$B_2 \rightarrow P_2$$

The reaction rates are given as:

$$R_1 = k_1 [B_1] \tag{4.22}$$

$$R_2 = k_2 [B_2] \tag{4.23}$$

The k values are given as:

$$k_1 = A_1 e^{(\frac{-Ea_1}{RT})} \tag{4.24}$$

$$k_2 = A_2 e^{(\frac{-Ea_2}{RT})} \tag{4.25}$$

The two reaction system above yields an overall reaction as follows:

$$B_{mix} \rightarrow P_{mix}$$

The overall reaction rate is given as:

$$R_{mix} = k_{mix} [B_{mix}] \tag{4.26}$$

$$B_{mix} = B_1 + B_2$$

For this simple case, linear combinations like equation 2.24 are used. Therefore the combined rate constant A_{mix} is found using a linear combination in equation 4.27.

$$ln(A_{mix}) = \sum x_i ln(A_i) \tag{4.27}$$

$$x_i = \frac{n_i}{\sum_{j=1}^{2} n_j}$$

The combined Ea_{mix} is found using equation 4.28.

$$Ea_{mix} = \sum x_i (Ea_i) \tag{4.28}$$

The combined $\triangle H_{rxn}$ is found using equation 4.29.

$$\triangle H_{rxn,mix} = \sum x_i (\triangle H_{rxn,i}) \tag{4.29}$$

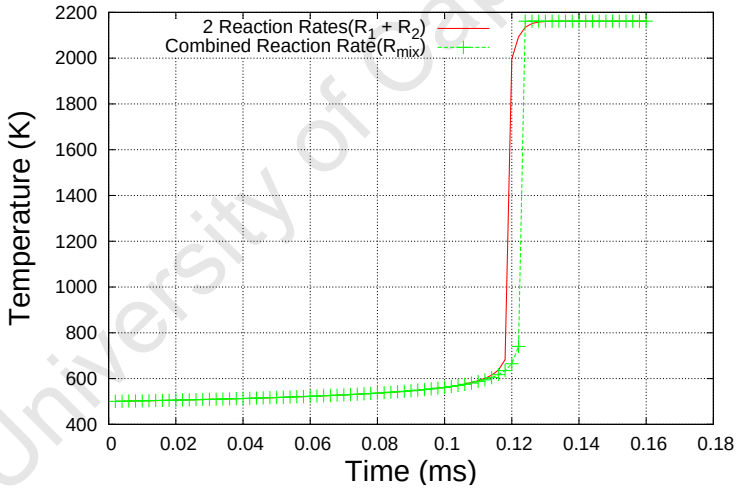

Figure 4.2: The temperature-time profiles are compared for the 2 reaction rates $(R_1 + R_2)$ and the blended single reaction rate (R_{mix}).

Figure 4.2 shows that the overall reaction was able to predict the two reaction system quite closely. The final temperature and the time of complete combustion are correct, but the temperature rise is slightly different. This is because a combined first order system will always have a sharp cut-off compared with the two reaction system which will always be more rounded. The same difference is seen in the concentration-time profiles in figure 4.3.

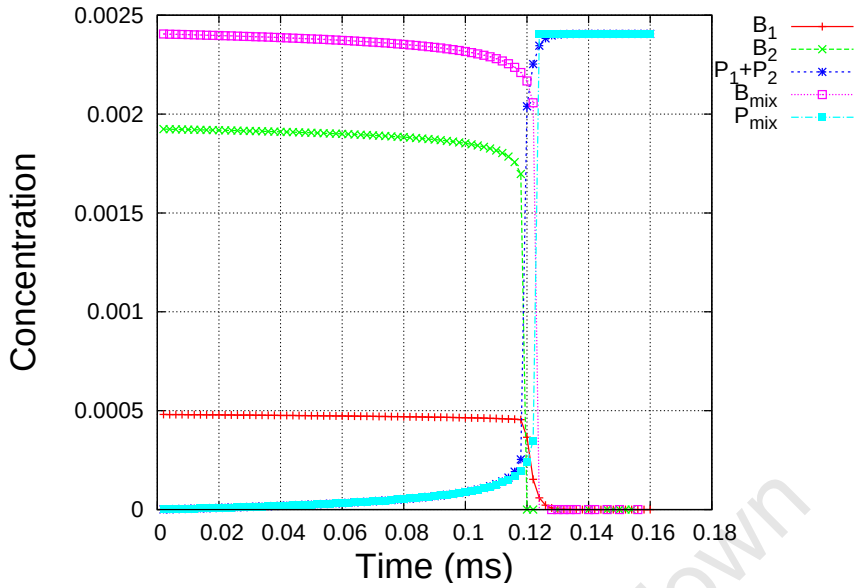

Figure 4.3: The concentration-time profiles are compared for the 2 reaction rates ($R_1 + R_2$) and the blended single reaction rate (R_{mix}).

These basic mixing rules break down when the reactions are no longer first order. It is however hypothesised that these basic mixing rules at least provide a first guess for dealing with higher order reactions.

4.4.2 Proposed Mixing Rules: High Temperature Kinetics

Using the conclusions made in section 4.4.1 as the starting point for obtaining blended constants, the model parameters A_{mix}, Ea_{mix} and $\triangle H_{rxn,mix}$ (where C is the number of fuels in the blend) for each reaction in the proposed models are:

$$ln(A_{mix}) = \sum_{i=1}^{C} x_i ln(A_i) \tag{4.30}$$

$$Ea_{mix} = \sum_{i=1}^{C} x_i (Ea_i) \tag{4.31}$$

$$\triangle H_{rxn,mix} = \sum_{i=1}^{C} x_i (\triangle H_{rxn,i}) \tag{4.32}$$

x_i is the fraction of fuel i in the fuel.

$$x_i = \frac{n_i}{\sum_{j=1}^{C} n_j}$$

The reactions in the proposed generalised kinetic model are not first order and consequently using these simple mixing rules was found to be unsatisfactory. Therefore additional binary interaction functions are needed to account for these discrepancies. Using the Peng-Robinson binary mixing rules as a basis, the following mixing rules are proposed.

$$f_A(x_i, x_j) = x_i^{n_{ij}} x_j^{2-n_{ij}} w_{ij} \tag{4.33}$$

$$f_{Ea}(x_i, x_j) = x_i^{ne_{ij}} x_j^{2-ne_{ij}} we_{ij} \tag{4.34}$$

The binary interaction constants for calculating the binary interaction function between fuel i and fuel j in reaction 1 are $n_{1,ij}$ and $w_{1,ij}$ for A_{mix} and $ne_{1,ij}$ and $we_{1,ij}$ for Ea_{mix}.

Therefore the model parameters A_{mix}, Ea_{mix} and $\triangle H_{rxn,mix}$ (where C is the number of fuels in the blend) are found using the following equations:

$$ln(A_{mix}) = \sum_{i=1}^{C} x_i ln(A_i) + \sum_{i=1}^{C-1} \sum_{j=i+1}^{C} f_A(x_i, x_j) \tag{4.35}$$

$$Ea_{mix} = \sum_{i=1}^{C} x_i (Ea_i) + \sum_{i=1}^{C-1} \sum_{j=i+1}^{C} f_{Ea}(x_i, x_j) \tag{4.36}$$

The heat of reaction did not require a binary interaction function, so it remains the basic mixing rule.

$$\triangle H_{rxn,mix} = \sum_{i=1}^{C} x_i (\triangle H_{rxn,i}) \tag{4.37}$$

4.4.3 Proposed Mixing Rules: Low Temperature Kinetics

The starting point for obtaining the blended model parameters A_{mix}, Ea_{mix} and $\triangle H_{rxn,mix}$ for the low temperature kinetics are the same as for the high temperature kinetics except for the fuel fractions that are used. y_i which the mole fraction of fuel i in the fuels with low temperature kinetics is used instead of x_i. C_L is the number of fuels with low temperature kinetics in the blend.

$$y_i = \frac{n_i}{\sum_{j=1}^{C_L} n_j}$$

$$ln(A_{mix}) = \sum_{i=1}^{C_L} y_i ln(A_i) \tag{4.38}$$

$$Ea_{mix} = \sum_{i=1}^{C_L} y_i (Ea_i) \tag{4.39}$$

$$\triangle H_{rxn,mix} = \sum_{i=1}^{C_L} y_i (\triangle H_{rxn,i}) \tag{4.40}$$

As in the high temperature kinetics, the low temperature kinetics are not first order and consequently using the simple mixing rules above was found to be unsatisfactory. Therefore additional binary interaction functions are needed to account for these discrepancies. So when both fuel i and fuel j have low temperature kinetics the mixing rules are fundamentally the same as for the high temperature kinetics.

$$f_A(y_i, y_j) = y_i^{n_{ij}} y_j^{2-n_{ij}} w_{ij} \tag{4.41}$$

$$f_{Ea}(y_i, y_j) = y_i^{ne_{ij}} y_j^{2-ne_{ij}} we_{ij} \tag{4.42}$$

Difficulties arise in the proposed mixing rules when finding the parameters for the low temperature kinetics for binary mixtures involving a fuel with and a fuel without low temperature kinetics. Fuels without low temperature kinetics (eg. methanol) do not have values for the pre-exponent rate constant A_i, Ea_i and $\triangle H_{rxn,i}$ for the low temperature reactions. The values of A_i, Ea_i and $\triangle H_{rxn,i}$ from the fuel with low temperature kinetics have to be used as the basis for the blended model parameters A_{mix}, Ea_{mix} and $\triangle H_{rxn,mix}$.

Using the Peng-Robinson binary mixing rules as a basis, the following binary mixing rules were proposed for blend fuel i, which has low temperature kinetics, and fuel j, which has no low temperature kinetics.

$$fSP_A(x_i, y_j) = y_j x_i^{n_{ij}} w_{ij} \tag{4.43}$$

$$fSP_{Ea}(x_i, y_j) = y_j x_i^{ne_{ij}} we_{ij} \tag{4.44}$$

x_i is the mole fraction of fuel i in the total fuel and y_j is the mole fraction of fuel j in the fuels with low temperature kinetics.

Therefore the model parameters A_{mix} and Ea_{mix} for the low temperature kinetics are found using the following:

$$ln(A_{mix}) = \sum_{i=1}^{C_L} y_i ln(A_i) + \sum_{i=1}^{C_L} \sum_{j=i+1}^{C} \begin{cases} if\ fuel\ i\ has\ low\ temperature\ kinetics & f_A(y_i, y_j) \\ else & fSP_A(x_i, y_j) \end{cases} \tag{4.45}$$

$$Ea_{mix} = \sum_{i=1}^{C_L} y_i (Ea_i) + \sum_{i=1}^{C_L} \sum_{j=i+1}^{C} \begin{cases} if\ fuel\ i\ has\ low\ temperature\ kinetics & f_{Ea}(y_i, y_j) \\ else & fSP_{Ea}(x_i, y_j) \end{cases} \tag{4.46}$$

4.5 Data to be used for Empirical Modelling

4.5.1 Experimental Data

Experimentally it is very difficult to obtain the temperature time profile for combustion in any system and in most cases the experiments are limited to low pressures and then only cover a small range of conditions (Schreiber et al., 1994). This is one of the main reasons that most models are based on measured ignition delay data. Minetti et al. (1995) obtained composition profiles for the combustion of n-heptane in a rapid compression machine and Vanhove et al. (2006) obtained single and binary concentration-time profiles in rapid compression machines.

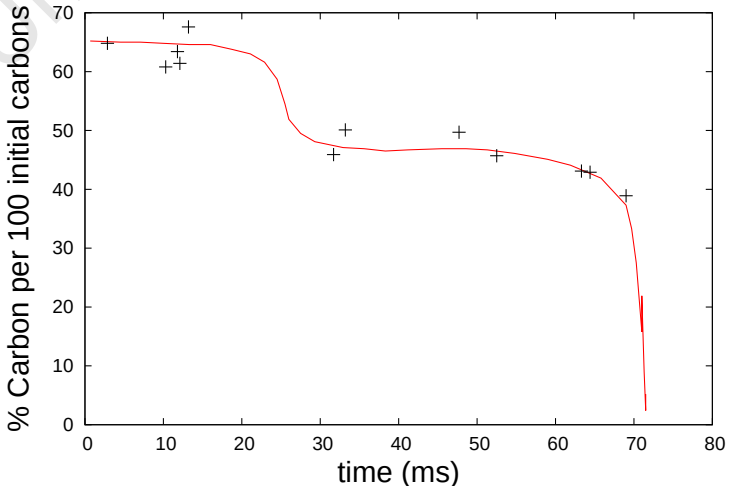

Figure 4.4: i-Octane profile during the autoignition delay of the 65/35 i-octane/toluene mixture at initial conditions of Tc=700 K and P=16.6 bar. (Vanhove et al., 2006) Study was done in a RCM.

4.5.2 CHEMKIN Time Series Data

The CHEMKIN Collection (Version 3.7) is a powerful software system for solving complex chemical kinetics problems. It was originally developed for gas phase combustion problems and has become standard in combustion modelling for describing all the chemical reactions, their rate parameters and the thermodynamic and transport properties of species. For the simulation of each fuel, CHEMKIN requires detailed chemical mechanisms which are available from various sources in the literature.

The rate constants of the proposed model C were regressed using results from more comprehensive kinetic models simulated in CHEMKIN. The detailed chemical kinetic mechanisms were obtained from Curran et al. (1998) for n-heptane and Curran et al. (2002) for i-octane.

Temperature-time profiles and the resulting ignition delay diagram were used to derive the model. It was initially thought to use the composition profiles as well. This was abandoned due to adding too many complexities and doubts over the validity of the the composition profiles.

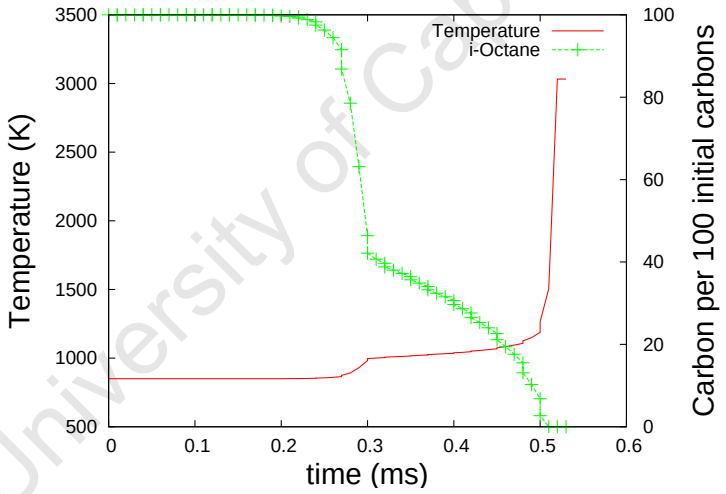

Figure 4.5: Temperature profile and mole fraction profile of i-octane, for the combustion of i-octane in a combustion bomb, as simulated by CHEMKIN. Simulation at initial conditions: 700K and 20 bar.

The experimental data found in figure 4.4 shows that the composition profiles from the CHEMKIN simulations in figure 4.5 are perhaps not accurate. The experimental setup for the data obtained in figure 4.4 is different in many respects to the settings modelled in CHEMKIN to obtain the data seen in figure 4.5. And as a result there are, as expected, both significant quantitative differences in the composition profiles, as well as in the ignition delay. Qualitatively the composition profiles of i-octane should be similar, which they are not. In figure 4.4 the experimental data shows roughly 30% of the i-octane consumed in the 'cool' flame while the CHEMKIN data shows roughly 60%

consumed in figure 4.5. This could perhaps be accounted for by the experimental data coming from an i-octane, toluene mixture. A far more conclusive observation is that there is essentially no consumption of the fuel from after the 'cool' flame until the 'hot' ignition in figure 4.5. CHEMKIN predicts that the fuel continues to be consumed in the second ignition delay and is essentially consumed (around 70%) before the final ignition. This cannot be accounted for by the experimental data coming from a blend.

It was considered that CHEMKIN distinguishes between i-octane and its radicals while the gas chromatography and other techniques used by Vanhove et al. (2006) might not. However, looking at the CHEMKIN data, the cumulative C_8H_{17} radicals do not exceed a mole fraction of 10^{-6} at any point, making their contribution negligible. This means that although CHEMKIN has been validated for ignition delay diagrams (Viljoen et al., 2005), the model has not been validated for the time series data, the composition profiles nor the temperature profiles. This means that analyses of the composition profiles produced by CHEMKIN might not be as helpful in developing a reduced model as first thought.

Whether or not the temperature-time profiles can be used to base the model on is also in doubt until good experimental temperature-time profiles can be found in the literature to validate them. However until then, a generalised model that can model a highly detailed mechanism would be a step toward modelling experimental data. If the generalised model can accurately reproduce the detailed model it will be a useful tool in CFD calculations. The principles developed in this paper can be readily applied to experimental data once it becomes available.

4.6 Parameter Fitting

The model parameters were regressed using data from comprehensive kinetic models of alkane oxidation which were solved using CHEMKIN. The detailed chemical kinetic mechanisms were obtained from Curran et al. (1998) for n-heptane and Curran et al. (2002) for i-octane. The CHEMKIN data was generated at the Sasol Advanced Fuel Laboratory using the CHEMKIN simulation package.

The system of non-linear, initial value problems containing ordinary differential equations were solved with DDASAC (Caracotsios and Stewart, 1995) integration package, which uses the implicit integrator DDASSL (Brennan et al., 1989; Petzold, 1982). DDASAC also has a sensitivity analysis function which solves the first-order parametric sensitivities.

4.6.1 Parameter Estimation using GREG

The pre-exponent factor A_i and the activation energy Ea_i for each reaction were taken as the adjustable parameters in the model.

$$k_i = A_i * e^{\frac{Ea_i}{RT}} \tag{4.47}$$

FORTRAN 77 package GREG (Stewart et al., 1992) was used to carry out the least squares minimisation of the errors between the proposed model and the detailed model, normalised to the values of the detailed model, equation 4.48. The initial guess for the parameters was obtained by manually adjusting the parameters to yield a response with a similar shape to the actual data. GREG was then used to further refine these parameters.

$$S(\theta) = \sum_{u=1}^{NOB} \left[1 - \frac{F(T0_u)}{Y_u}\right]^2 \tag{4.48}$$

$S(\theta)$ is the objective function which is minimised to fit proposed model's prediction of the ignition delay diagram with the data from CHEMKIN. θ is the vector of temperatures at which the ignition delay are predicted. NOB is the number of observations, in other words the number of data points. Y is the vector of CHEMKIN data points against which the model parameters are being regressed. $F(T0_u)$ is the model prediction of the ignition delay at starting temperature $T0_u$.

4.6.2 Parameter Estimation using the Genetic Algorithm (GA)

The GA was used as an alternative to GREG to refine the model parameters, where pre-exponent factor A_i and the activation energy Ea_i for each reaction were taken as the adjustable parameters in the model. The initial guess for the parameters was obtained by manually adjusting the parameters to yield a response with a similar shape to the actual data. Then the GA minimised the objective function, equation 4.48.

The GA used in this study was developed by Carroll (1996) to model chemical lasers.

4.7 Regression Analysis

The following regression analysis was obtained from the least squares minimisation and is therefore based on linear systems and a normalised error distribution is implicitly assumed. Therefore the results obtained can only be taken as a first approximation. Proper analysis of non-linear models can only be obtained by performing a non-parametric analysis such as the bootstrap analysis.

The accuracy of the model is assessed using the standard error of the parameters, the standard error of the responses and the correlation between the parameters. These are obtained using the standard error, the Jacobian matrix and the covariance matrix.

Standard error is calculated as follows:

$$s = \sqrt{\frac{S(\hat{\theta})}{N}}, \tag{4.49}$$

where N is the number of data points and $S(\hat{\theta})$ is the normalised objective function, equation 4.48.

The Jacobian matrix is defined by equation 4.51.

$$J = \frac{\partial(f(x_i, \theta)}{\partial \theta_j} \tag{4.50}$$

The Jacobian matrix can also be used to look at the sensitivity of the model's prediction at a certain point to each parameter. This sensitivity analysis can be used where the different parameters are significant or dominant.

The covariance matrix is defined by equation 4.51.

$$Cov = \left\{J^T J\right\}^{-1} \tag{4.51}$$

4.7.1 Standard Errors of Parameters

The standard error associated with parameter θ_p can be calculated using equation 4.52.

$$SE_{parameter}(\theta_p) = s\sqrt{Cov_{p,p}} \tag{4.52}$$

4.7.2 Standard Errors of Predictions

The standard error of prediction associated with data point q_m can be calculated using equation 4.53.

$$SE_{prediction}(q_m) = s\sqrt{j_m^T Cov j_m} \tag{4.53}$$

where j_m is a single row from the Jacobian matrix, defined as follows:

$$j_m = \frac{\partial(j(q_m, \theta_i)}{\partial \theta_i} \tag{4.54}$$

4.7.3 Parameter Correlation

The square symmetrical correlation matrix is obtained by normalising the covariance matrix with respect to the parameter variances, as shown in equation 4.55. 0 indicates no correlation and 1 indicates complete correlation between the two parameters. A correlation of 0 to 0.4 is typically considered as acceptable.

$$Cor = W.C.W \tag{4.55}$$

where W given by the square root of the Jacobian diagonal.

$$W = \begin{bmatrix} \sqrt{C_{1,1}} & \cdots & 0 & \cdots & 0 \\ \vdots & \ddots & & & \vdots \\ 0 & & \sqrt{C_{i,i}} & & 0 \\ \vdots & & & \ddots & \vdots \\ 0 & \cdots & 0 & \cdots & \sqrt{C_{P,P}} \end{bmatrix}$$

A high correlation between parameter means that the 'relationship' between the parameters rather the actual parameters has been regressed to fit the data. It is not a measure of the prediction's validity but rather an indication that the parameter values could be very wrong and that the number of model parameters could be reduced. Reaction rate parameters often exhibit a high degree of correlation (Elliott et al., 2004).

Chapter 5

Results and Discussion

5.1 Pure Fuels

The combustion of all the pure fuels were simulated at 20, 30 and 40 bar and at a stoichiometric ratio with air.

5.1.1 n-Heptane

Table 5.1: Parameters for n-heptane used in Model C

Reaction No.	$\triangle H_{rxn}$	A	$\frac{E_a}{R}$	Pressure constant
	kJ/mol	Reaction specific	K	
C1	-709.9	1.69×10^6	18.7×10^3	-1.00
C2	4709.0	1.00×10^8	1.00×10^3	
C3	20.0	4.78×10^5	12.7×10^3	-0.50
C4+	20.0	2.66×10^{13}	21.3×10^3	-1.40
C4-	-20.0	2.25×10^{23}	37.9×10^3	
C5	4000.0	4.64×10^{14}	18.9×10^3	

The pressure constants were regressed with the other coonstants to predict the variation in ignition behaviour caused by pressure for n-heptane. The same pressure constants are used for different fuels as was done in the Schreiber model (Schreiber et al., 1994).

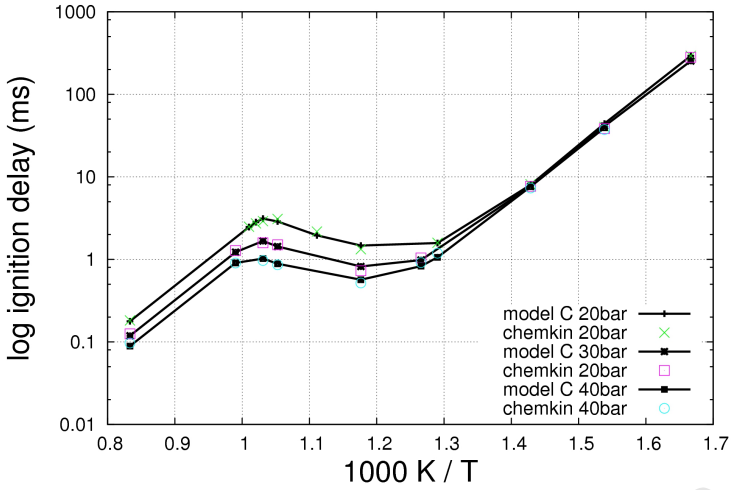

Figure 5.1: n-Heptane ignition delay diagrams at various pressures (20, 30 and 40 bar)

The temperature-time profiles were only regressed until full consumption of the fuel or alternatively until the final temperature was reached.

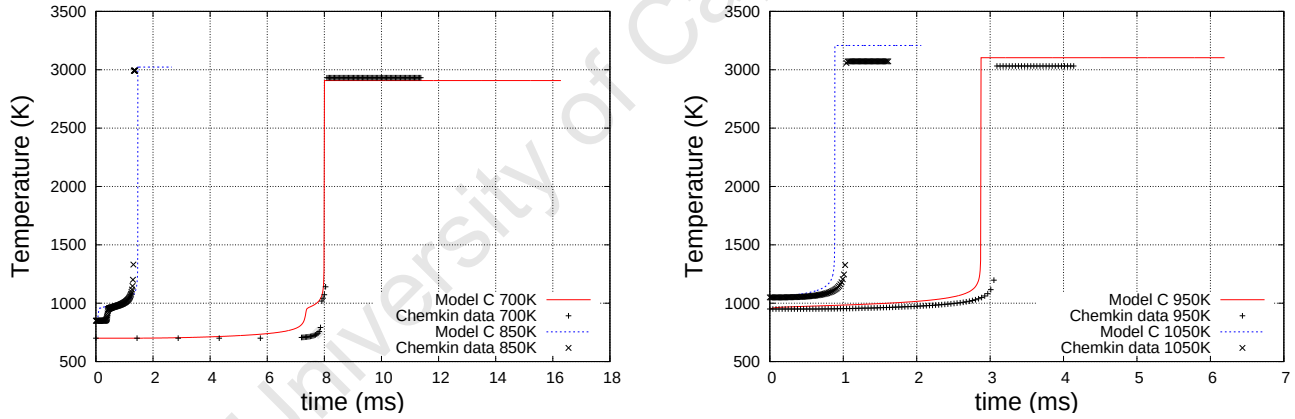

(a) Initial temperature at 700K and 850K

(b) Initial temperature at 950K and 1000K

Figure 5.2: n-Heptane temperature-time profiles using Model C at 20 bar

Figure 5.1 shows that the model C fits the ignition delay diagram for n-heptane well. However the temperature-time profiles starting at 700K and 850K in figure 5.2a show that the two stage ignition has not been accurately predicted. This is because once the initial ignition has taken place model C is not able to predict the short second ignition delay which is predicted by CHEMKIN. Therefore when the parameters were solved to fit the ignition delay, the first ignition is predicted earlier in order for the final ignition delay to be correct. This effect is achieved by adjusting numerous parameters (A_3, A_{4+}, A_{4-}, Ea_3, Ea_{4+}, Ea_{4-}). All the parameters need to be adjusted as they are highly correlated as shown in figures 5.4, 5.5 and 5.6.

Model C's inability to predict the shorter second ignition delay is due to insufficient chemical feedback, otherwise stated as insufficient chemical interaction between the low temperature kinetics and the high temperature kinetics. Yates and Viljoen (2008) had a similar problem with their model (discussed in section 2.3.5) which they worked around by using a multiplying 'X' factor to account for the chemical feedback their model was unable to provide.

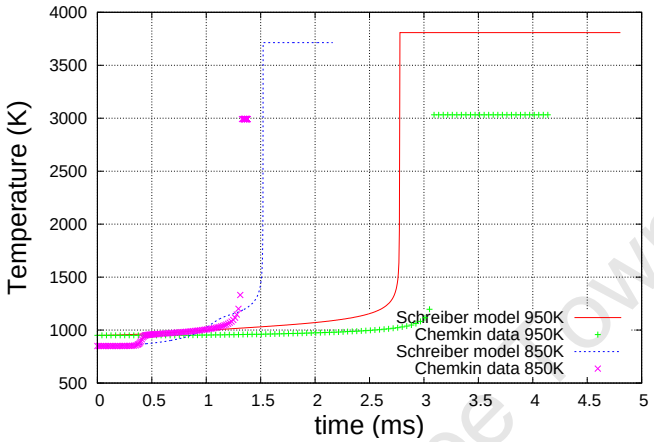

Figure 5.3: Temperature profiles comparing the Schreiber model to CHEMKIN simulation data (using detailed kinetics from Curran et al. (1998)) for the combustion of n-Heptane in a combustion bomb at 20 bar two initial temperatures, 850K and 950K.

Although the temperature profiles are not predicted accurately, the predictions are better than those predicted by the Schreiber model (figure 5.3) in terms of the low temperature gradient in the delay before the 'cool' flame and the delay before final ignition.

5.1.1.1 Regression Analysis

Table 5.2: Parameter Standard Error for n-heptane

Reaction No.	A	Standard Error	Relative Standard Error	$\frac{E_a}{R}$	Standard Error	Relative Standard Error
	Reaction specific			K		
C1	1.69×10^6	3.93×10^4	0.023	18.7×10^3	5.29×10^2	0.020
C2	1.00×10^8	-	-	1.00×10^3	-	-
C3	4.78×10^5	1.85×10^4	0.047	12.7×10^3	5.12×10^2	0.028
C4+	2.66×10^{13}	7.72×10^{11}	0.039	21.3×10^3	1.06×10^3	0.042
C4-	2.25×10^{23}	8.24×10^{21}	0.030	37.9×10^3	1.89×10^3	0.040
C5	4.64×10^{14}	9.11×10^{12}	0.037	18.9×10^3	5.70×10^2	0.050

Reaction C2 is purely chemically driven, so the constants for reaction C2 are chosen to make sure that it remains chemically driven and therefore not involved in the model fitting process. Therefore the pre-exponent rate constant A_2 and activation energy Ea_2 are not regressed for in the parameterisation process and therefore not included in the correlation analysis which follows.

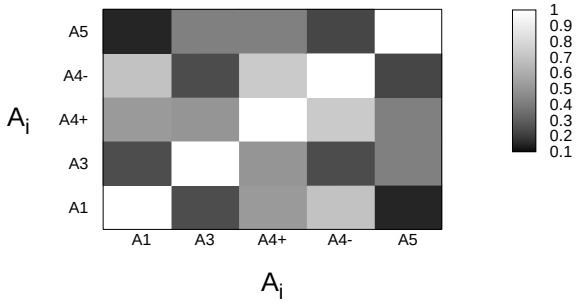

Figure 5.4: Correlation factors for pre-exponent rate constants A_i in Model C.

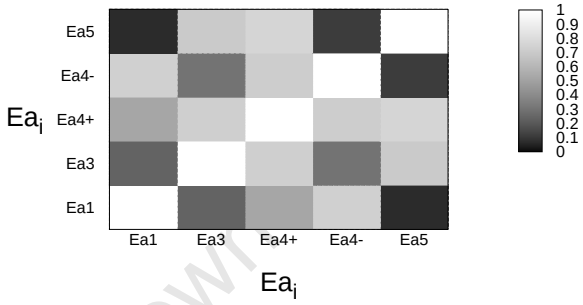

Figure 5.5: Correlation factors for activation energies Ea_i in Model C.

The correlation factors of 1.0 diagonally across the figures 5.4 and 5.5 are the correlation of the parameters with themselves which is always 1.0 by definition.

Figures 5.4 and 5.5 both show that the constants of reactions C3, C4+, C4- and C5 all have correlations over 0.4. This was expected due to all of the reactions being part of the low temperature kinetics and the expectation of high correlation within reaction parameters. The high correlation means that the model optimisation by the genetic algorithm did not only regress for the parameters but also for the relationship between the parameters. The lack of correlation between the constants of reaction C1 in the high temperature kinetics and the reactions in the low temperature kinetics is expected due to the distinct temperature regions they operate in.

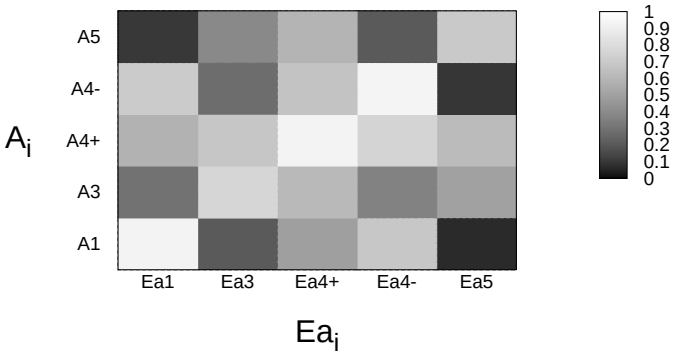

Figure 5.6: Correlation factors of pre-exponent rate constants A_i with activation energies Ea_i in Model C.

As expected, the correlations between each reaction's pre-exponent rate constants A_i and activation energies Ea_i are very high as seen in figure 5.6.

The high correlation factors for the parameters of model C could explain why GREG, which uses Least Squares optimisation, found it difficult to solve the system satisfactorily.

5.1.1.2 Sensitivity Analysis

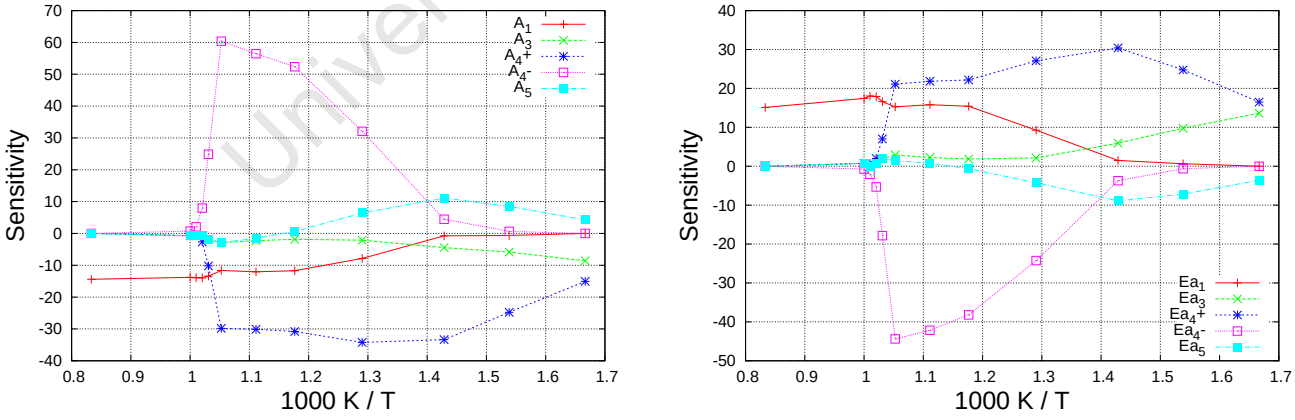

(a) Pre-exponent rate constants A_i

(b) Activation energies Ea_i

Figure 5.7: Sensitivity analysis of Model C at 20 bar

As expected, the rate constants in the low temperature kinetics, seen in figures 5.7a and 5.7b, are very sensitive below 1000K and insensitive above 1000K when the high temperature kinetics dominate (Reaction C1). In the NTC region it is the rate constants for reaction C4- which are

the most sensitive. The importance of the NTC region means the rate constants for reaction C4- are the most important parameters in the regression process. The sensitivity of the parameters at different temperature regions means that data across the full temperature range is needed to regress all the parameters.

In figure 5.7a, the sensitivity of A_1, A_3 and A_{4+} is negative because an increase of these constants results in a shorter ignition delay. The opposite is true for A_{4-}, because an increase in its value speeds up the reverse reaction C4- which increases the ignition delay. Perhaps unexpectedly, A_5 also has a positive sensitivity. This is because if reaction C5 is too fast it depletes the radical 'I' too quickly and it slows the build up of the radicals to the critical concentration necessary for ignition. Which means that an increase in A_5 also increases the ignition delay.

The sensitivities of the activation energies, Ea_i, in figure 5.7b are very similar to those of the pre-exponent rate constant, A_i, in figure 5.7a, except that the sensitivities are reversed. Increasing the activation energy of a reaction delays the reaction compared to an increase in the pre-exponent rate constant which expedites the reaction. The similarity of the absolute sensitivities of Ea_i and A_i again illustrate the correlation seen in figure 5.6.

5.1.1.3 Final Temperatures

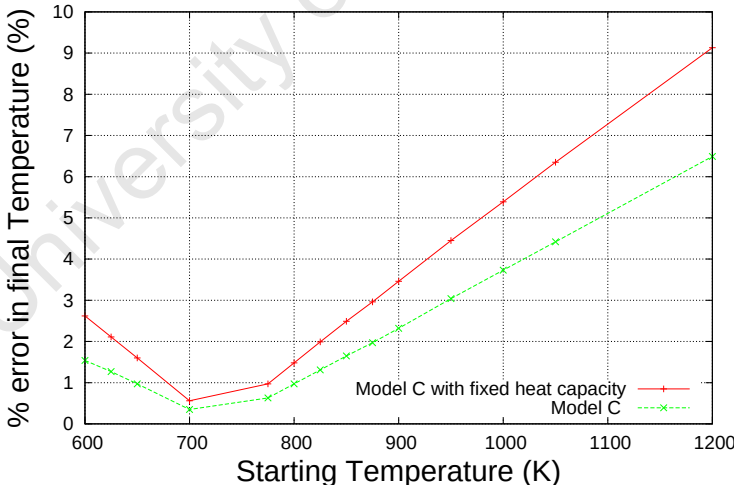

Figure 5.8: Percentage error of the final temperature for model C, with constant heat capacity and a temperature/species dependent heat capacity

Although the prediction of the final temperature is not the aim of this work, it can be seen from figure 5.8 that the prediction of the final temperature is not accurate. Figure 5.8 shows the accuracy of the final temperature of the model C when it uses a constant heat capacity for the system compared with when model C uses a temperature and species dependent heat capacity.

The temperature and species dependent heat capacity does increase the accuracy of the final temperature, but the error is still significant.

5.1.2 i-Octane

Model D is the proposed model for i-octane, which is adapted from Model C, which is the proposed model for n-heptane. Table 5.3 contains the regressed parameters for Model D, which is described in sub-section 4.3.4.

Table 5.3: Parameters for i-octane used in Model D

Reaction No.	$\triangle H_{rxn}$	A	$\frac{E_a}{R}$	Pressure constant
	kJ/mol	Reaction specific	K	
D1	-709.9	7.50×10^5	17.6×10^3	-1.00
D2	5209.0	1.0×10^7	1.0×10^3	
D3	20.0	1.00×10^5	10.7×10^3	-0.50
D4+	20.0	3.24×10^{13}	24.4×10^3	-1.40
D4-	-20.0	2.13×10^{23}	37.7×10^3	
D5	4500.0	6.00×10^{15}	26.0×10^3	

Model D and its regressed parameter values were able to predict the ignition delay diagrams which are compared to the ignition delay diagrams from the CHEMKIN simulations in figure 5.9. The temperature-time profiles predicted by model D are also compared to those predicted by the CHEMKIN simulation in figure 5.10a and figure 5.10b.

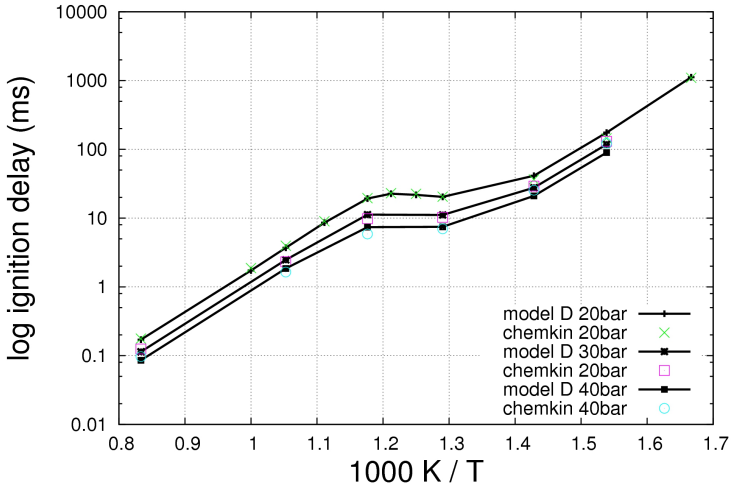

Figure 5.9: i-Octane ignition delay diagrams using Model D at various pressures (20, 30 and 40 bar)

The temperature-time profiles were only regressed until full consumption of the fuel or alternatively until the final temperature was reached.

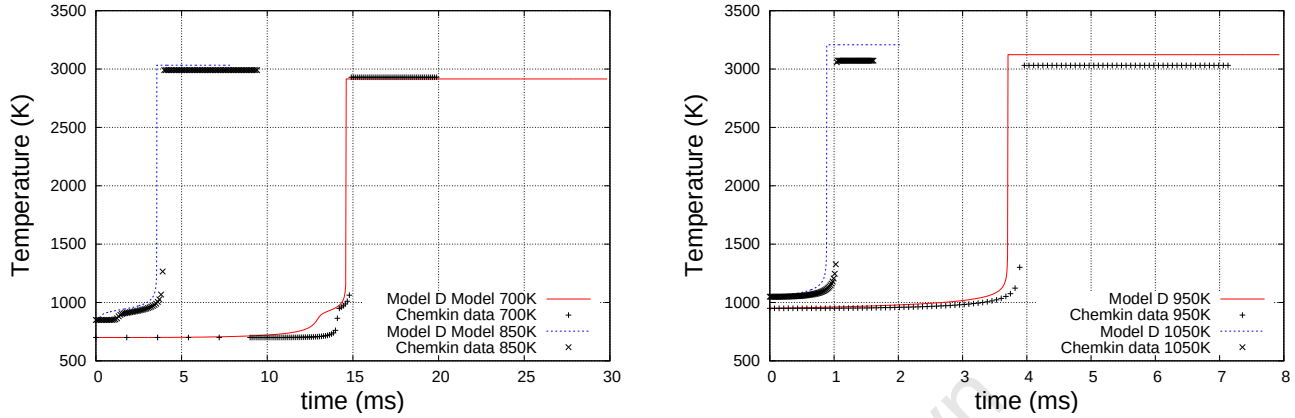

(a) Starting temperatures at 700K and 850K

(b) Starting temperatures at 950K and 1050K

Figure 5.10: i-Octane temperature-time profiles using model D at 20 bar

Figure 5.9 shows that the model D fits the ignition delay diagram for i-octane very well. As with the model C, model D cannot predict a short enough second ignition delay so the 'cool' flame is predicted earlier so that the overall ignition delay is correctly predicted.

5.1.2.1 Regression Analysis

Table 5.4: Parameter Standard Error for i-octane

Reaction No.	A	Standard Error	Relative Standard Error	$\frac{E_a}{R}$	Standard Error	Relative Standard Error
	Reaction specific			K		
D1	7.50×10^5	2.99×10^4	0.040	17.6×10^3	1.52×10^2	0.033
D2	1.0×10^7	-	-	1.0×10^3	-	
D3	1.00×10^5	1.21×10^4	0.135	10.7×10^3	9.93×10^2	0.086
D4+	3.24×10^{13}	2.49×10^{12}	0.121	24.4×10^3	1.77×10^3	0.084
D4-	2.13×10^{23}	2.24×10^{22}	0.077	37.7×10^3	2.73×10^3	0.093
D5	6.00×10^{15}	1.95×10^{14}	0.105	26.0×10^3	1.89×10^3	0.073

Reaction D2 is purely chemically driven, so the constants for reaction D2 are chosen to make sure that it remains chemically driven and therefore not involved in the model fitting process.

The standard errors of model D are comparable to those of model C. The sensitivity analysis, correlation factors and final temperature prediction of model D are very similar to those of model C and therefore not repeated.

5.1.3 Methanol

Model E is the proposed model for methanol, which is adapted from Model C, which is the proposed model for n-heptane. Table 5.5 contains the regressed parameters for Model E, which is described in sub-section 4.3.4.

Table 5.5: Parameters for methanol used in Model E

Reaction No.	$\triangle H_{rxn}$	A	$\frac{E_a}{R}$	Pressure constant
	kJ/mol	Reaction specific	K	
E1	-60.0	2.43×10^7	21.2×10^3	-1.00
E2	560.0	5.14×10^6	1.00×10^3	
E3	-	-	-	-
E4+	-	-	-	-
E4-	-	-	-	
E5	-	-	-	

Model E and its regressed parameter values were able to predict the ignition delay diagrams which are compared to the ignition delay diagrams from the CHEMKIN simulations in figure 5.11. The temperature-time profiles predicted by model E are also compared to those predicted by the CHEMKIN simulation in figure 5.12.

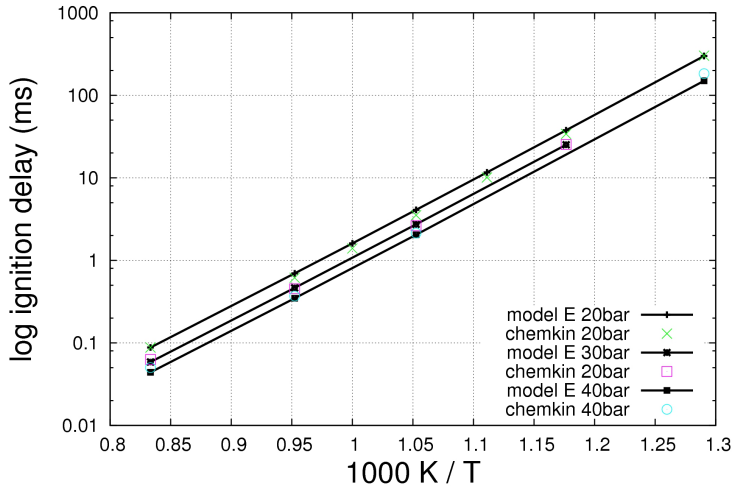

Figure 5.11: Methanol ignition delay diagrams at various pressures (20, 30 and 40 bar)

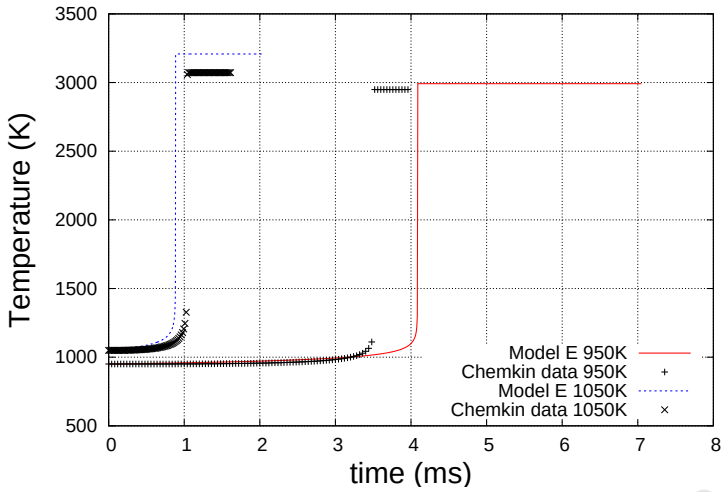

Figure 5.12: Methanol temperature time profiles starting at 950K and 1050K, at 20 bar

With no cool flame or NTC behaviour the ignition delay diagram is accurately predicted using only high temperature kinetics. This makes the model fitting an almost trivial task relative to the fuels with NTC behaviour.

Table 5.6: Parameter Standard Error for methanol

Reaction No.	A	Standard Error	Relative Standard Error	$\frac{E_a}{R}$	Standard Error	Relative Standard Error
	Reaction specific			K		
E1	2.43×10^7	1.04×10^6	0.043	21.2×10^3	3.76×10^1	0.002
E2	5.14×10^6	-	-	1.00×10^3	-	-

Reaction E2 is purely chemically driven, so the constants for reaction 2 are chosen to make sure that it remains chemically driven and therefore not involved in the model fitting process.

With only two parameters to be regressed for, the standard errors are understandably smaller than those for n-heptane and i-octane.

5.2 PRF Blends

The model used to predict the PRF blends between i-octane and n-heptane is obtained from a combination of model C and model D. An example of combining two models to obtain a blended model is given in section 7.1 in Appendix .

Table 5.7: Interaction parameters for pre-exponent rate constant A_i and activation energy $\frac{Ea_i}{R}$ for n-heptane/i-octane blend

	A_i		$\frac{Ea_i}{R}$	
Reaction No.	n	w	ne	we
1	1.39	-0.41	1.00	0.00
2	1.00	0.00	1.00	0.00
3	0.618	10.4	0.681	6470
4+	1.47	-2.38	1.38	-2160
4-	0.971	-1.79	1.99	371
5	0.740	4.11	1.88	1190

The combustion of all the blends were simulated at 20 bar and at stoichiometric ratios with air. The percentage composition is in terms of liquid volume. The ignition delay diagrams for pure n-heptane and i-octane are plotted as points of reference for each fuel blend.

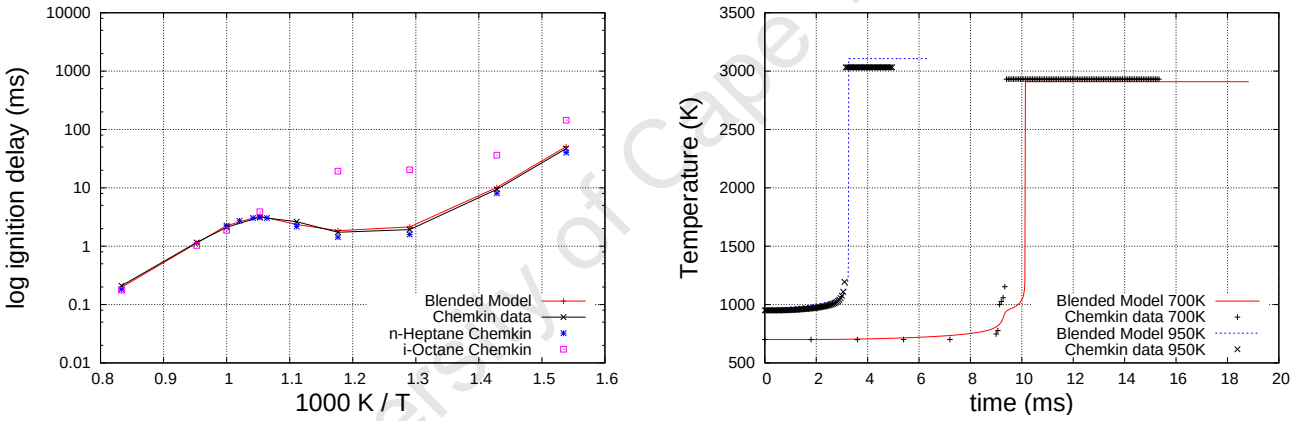

(a) Ignition delay diagram

(b) Temperature-time profiles

Figure 5.13: Binary blend, by liquid volume 20% i-octane and 80% n-heptane (18.2/81.8% mole)

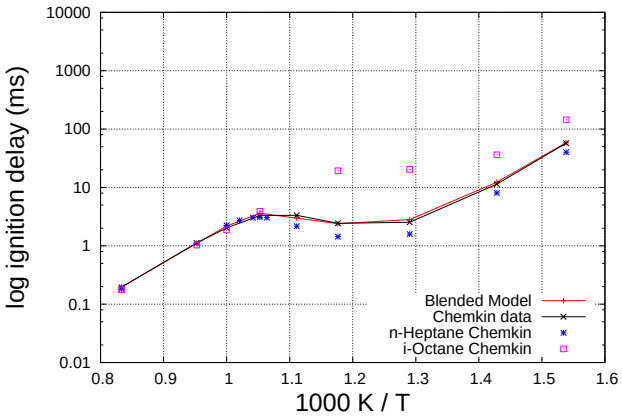

(a) Ignition delay diagram

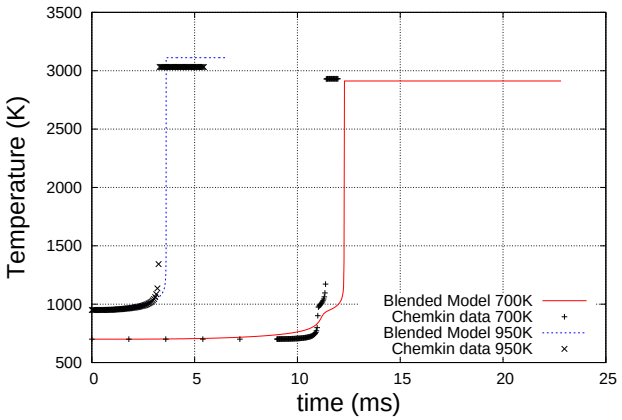

(b) Temperature-time profiles

Figure 5.14: Binary blend, by liquid volume 40% i-octane and 60% n-heptane (37.2/62.8% mole)

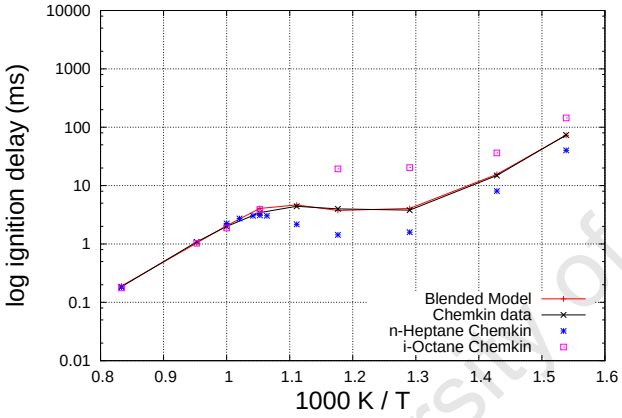

(a) Ignition delay diagram

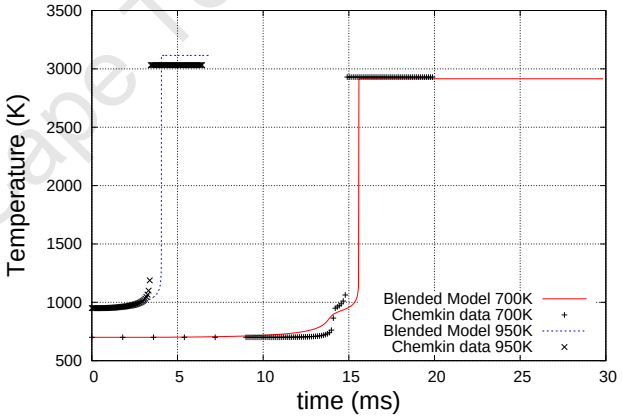

(b) Temperature-time profiles

Figure 5.15: Binary blend, by liquid volume 60% i-octane and 40% n-heptane (57.1/42.9% mole)

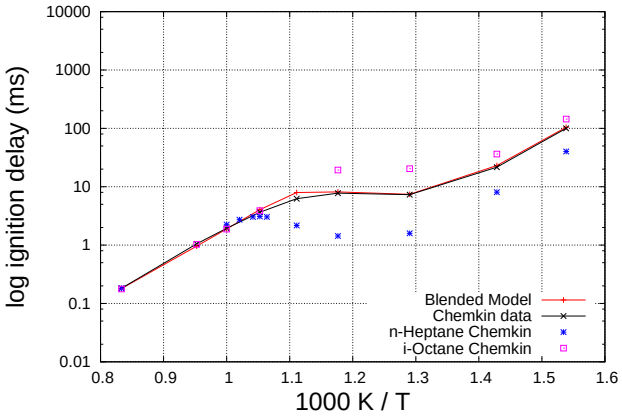

(a) Ignition delay diagram

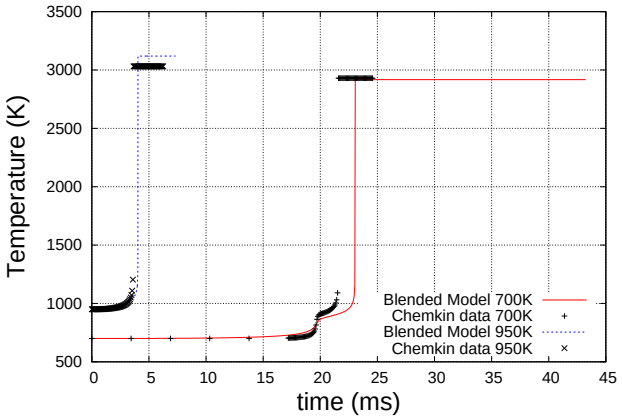

(b) Temperature-time profiles

Figure 5.16: Binary blend, by liquid volume 80% i-octane and 20% n-heptane (78.0/22.0% mole)

Overall the ignition delay diagrams of the PRF blends are well predicted. The quality of the prediction has a lot to do with both fuels being from the paraffin class and therefore the ignition delay behaviour of the two fuels being quite similar to start off with. As with the temperature profiles of pure n-heptane and i-octane, the temperature profiles of their blends do not accurately predict the 'cool' flame temperature rise and the second ignition delay.

5.3 Methanol and i-Octane blends

The model used to predict blends between i-octane and methanol is obtained from a combination of model D and model E. An example of combining two models to obtain a blended model is given in section 7.1 in Appendix A.

Table 5.8: Interaction parameters for pre-exponent rate constant A_i and activation energy $\frac{Ea_i}{R}$ for methanol/i-octane blend

	A_i		$\frac{Ea_i}{R}$	
Reaction No.	n	w	ne	we
1	0.89	-0.90	1.50	-690.00
2	1.00	0.00	1.00	0.00
3	5.90	-3.60	3.00	870.00
4+	40.00	-32.00	7.10	11000.00
4-	24.00	0.42	40.00	-580.00
5	1.00	0.00	1.00	0.00

As the percentage of methanol in the blend decreases, the NTC behaviour becomes progressively more pronounced, as seen in figures 5.17a, 5.18a, 5.19a and 5.20a. To accurately predict this behaviour the rate constants in the low temperature kinetics are adjusted according to the fuel composition using the binary interaction functions. The change in the values of the constants as a function of composition are plotted in figures 5.21 and 5.22. The decrease in NTC behaviour is caused by slowing down the production radical 'I' (by decreasing A_3 and $A_{4+}$and increasing Ea_3 and Ea_{4+}) and increasing the reverse reaction of radical 'I' back to fuel 'F' (by decreasing A_{4-} and increasing Ea_{4-}).

The combustion of all the blends were simulated at 20 bar and at stoichiometric ratios with air. The ignition delay diagrams for pure methanol and i-octane are plotted as points of reference for each fuel blend.

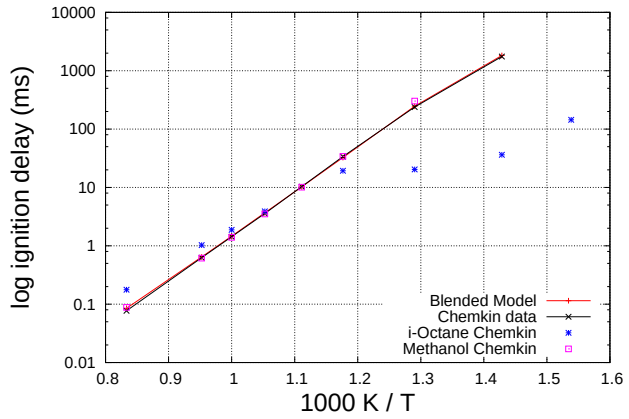

(a) Ignition delay diagram

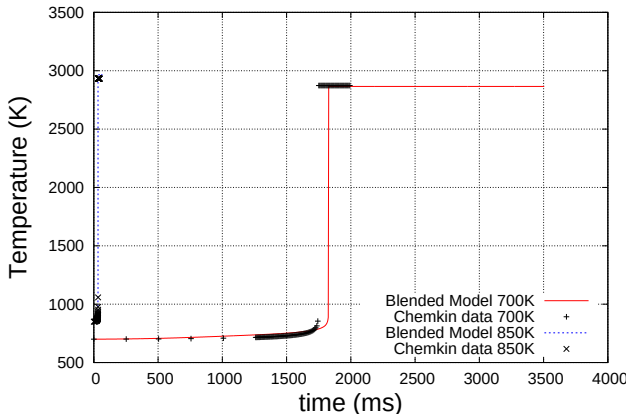

(b) Temperature-time profiles

Figure 5.17: Binary blend, by liquid volume 80% methanol and 20% i-octane (94.2/5.8% mole)

With a very low i-octane content, the low temperature kinetics of i-octane have little influence on the ignition delay of the blend.

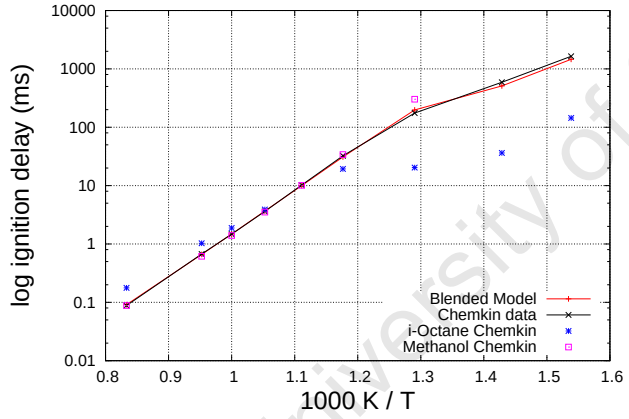

(a) Ignition delay diagram

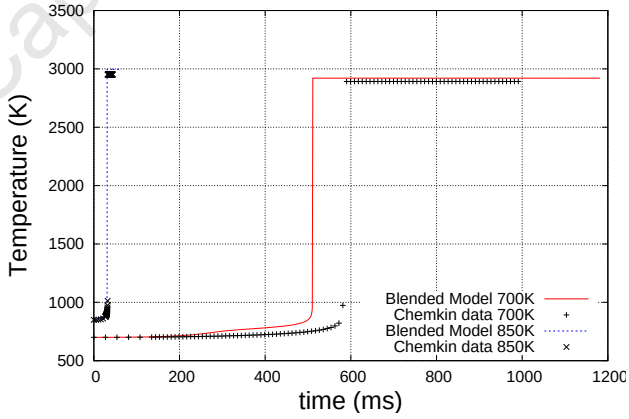

(b) Temperature-time profiles

Figure 5.18: Binary blend, by liquid volume 60% methanol and 40% i-octane (86.0/14.0% mole)

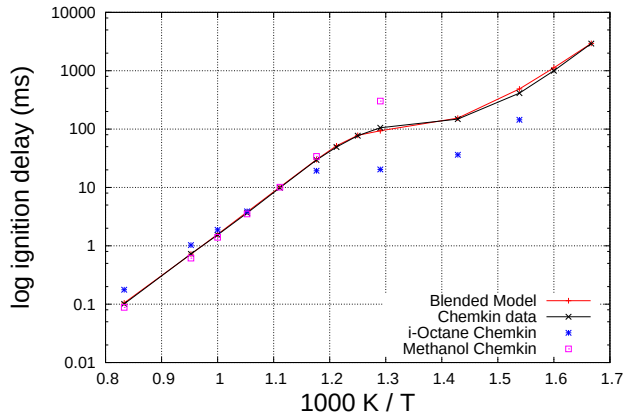

(a) Ignition delay diagram

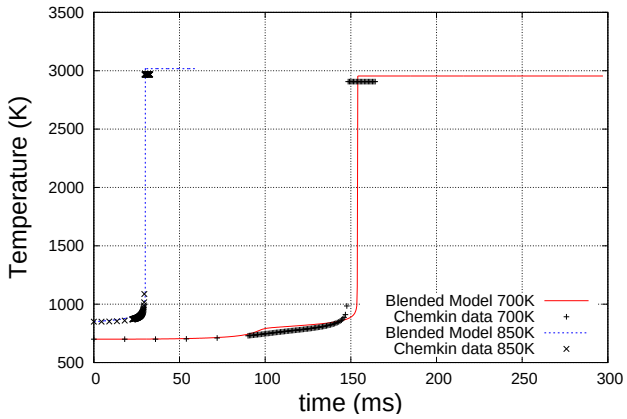

(b) Temperature-time profiles

Figure 5.19: Binary blend, by liquid volume 40% methanol and 60% i-octane (73.1/26.9% mole)

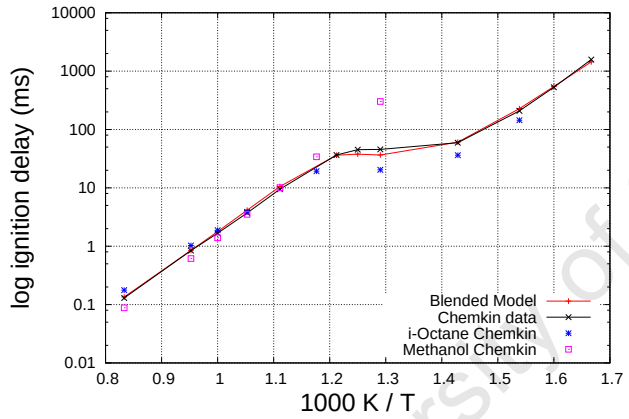

(a) Ignition delay diagram

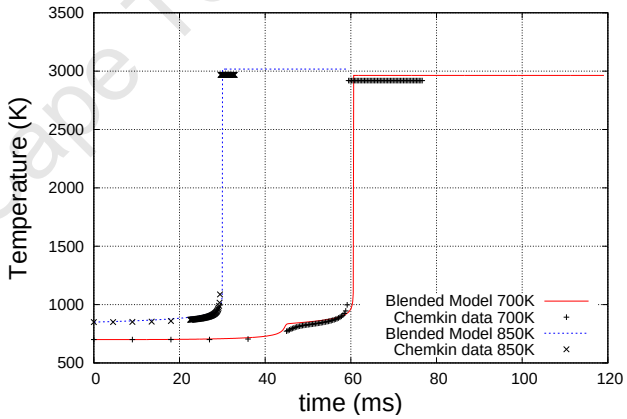

(b) Temperature-time profiles

Figure 5.20: Binary blend, by liquid volume 20% methanol and 80% i-octane (50.5/49.5% mole)

Overall the ignition delay diagrams of the methanol-octane blends are accurately predicted, considering the vast differences in ignition delay behaviour. However i-octane with less extreme NTC behaviour than n-heptane, is easier to model in combination with methanol. This is clearly seen when comparing the standard errors produced by the i-octane/methanol blends and the n-heptane/methanol blends.

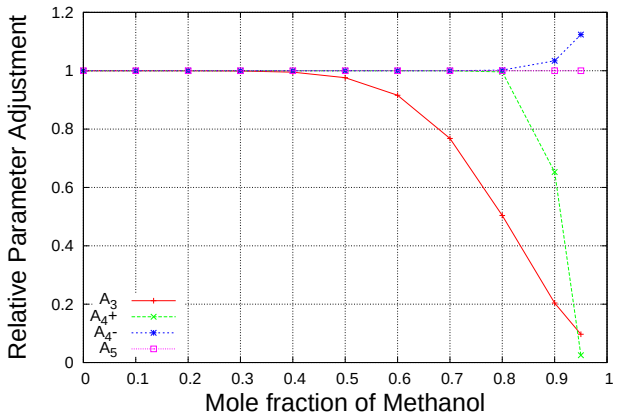

Figure 5.21: Pre-exponent rate constant A_i for i-octane/methanol blends, relative to A_i for i-octane (low temperature kinetics only).

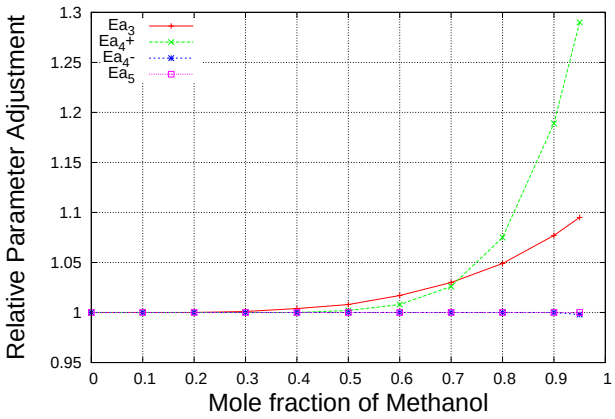

Figure 5.22: Activation energy Ea_i for i-octane/methanol blends, relative to Ea_i for i-octane (low temperature kinetics only).

5.4 Methanol and n-Heptane Blends

The model used to predict blends between i-heptane and methanol is obtained from a combination of model C and model E. An example of combining two models to obtain a blended model is given in section 7.1 in Appendix .

Table 5.9: Interaction parameters for pre-exponent rate constant A_i and activation energy $\frac{Ea_i}{R}$ for methanol/n-heptane blend

	A_i		$\frac{Ea_i}{R}$	
Reaction No.	n	w	ne	we
1	1.60	-4.40	1.70	-4000.00
2	1.00	0.00	1.00	0.00
3	23.00	-1.60	2.30	800.00
4+	19.0	-9.00	40.00	1800.00
4-	40.00	0.50	4.60	-900.00
5	1.00	0.00	1.00	0.00

In the i-octane/methanol blends, the rate constants in the low temperature kinetics were adjusted to predict the progressive decrease in NTC behaviour as the methanol content increased. The same adjustments are needed in the n-heptane/methanol blends except that the NTC behaviour of n-heptane is more extreme than that of i-octane. Therefore it was unexpected that the adjustments to the rate constants in the low temperature kinetics are less for the n-heptane/methanol blends than for the i-octane/methanol blends when comparing figures 5.23 and 5.24 to figures 5.21 and 5.22. The reason for this goes back to the high correlations between all the rate constants in the

low temperature kinetics (refer to figures 5.4, 5.5 and 5.6). When fitting parameters that are highly correlated it is their relationship which is fitted rather than the individual parameters.

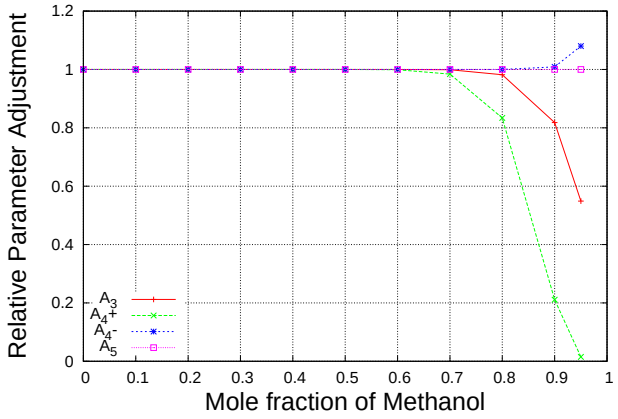

Figure 5.23: Pre-exponent rate constant A_i for n-heptane/methanol blends, relative to A_i for n-heptane (low temperature kinetics only).

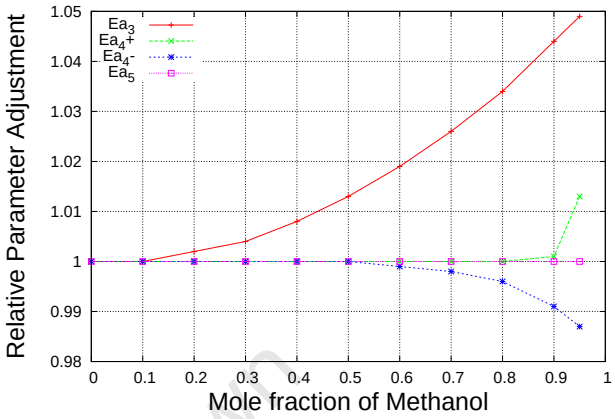

Figure 5.24: Activation energy Ea_i for n-heptane/methanol blends, relative to Ea_i for n-heptane (low temperature kinetics only).

The combustion of all the blends were simulated at 20 bar and at stoichiometric ratios with air. The ignition delay diagrams for pure n-heptane and methanol are plotted as points of reference for each fuel blend.

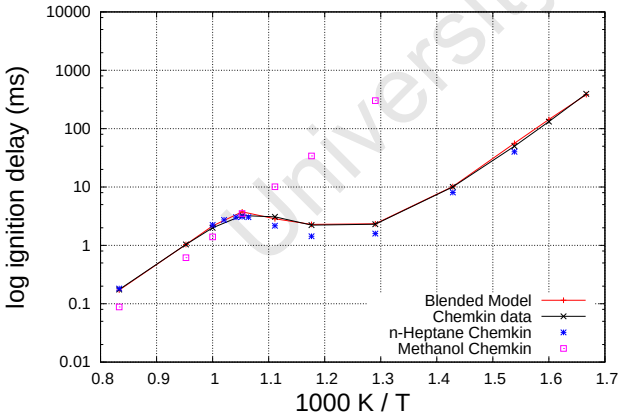

(a) Ignition delay diagram

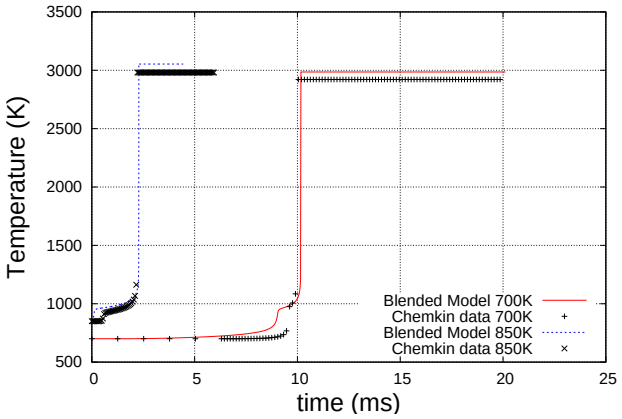

(b) Temperature-time profiles

Figure 5.25: Binary blend, by liquid volume 20% methanol and 80% n-heptane (47.5/52.5% mole)

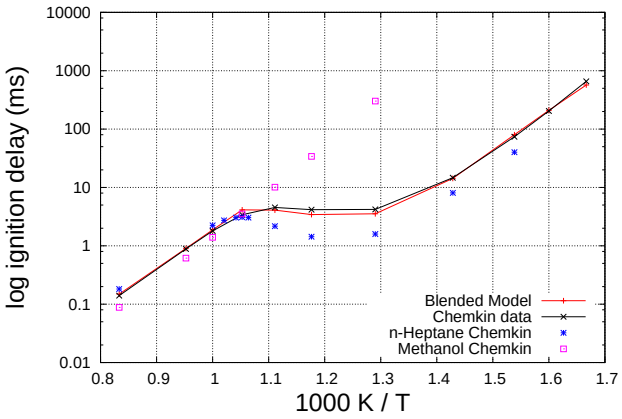

(a) Ignition delay diagram

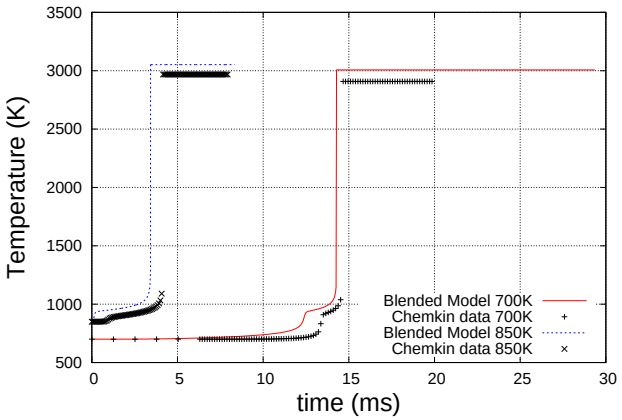

(b) Temperature-time profiles

Figure 5.26: Binary blend, by liquid volume 40% methanol and 60% n-heptane (70.7/29.3% mole)

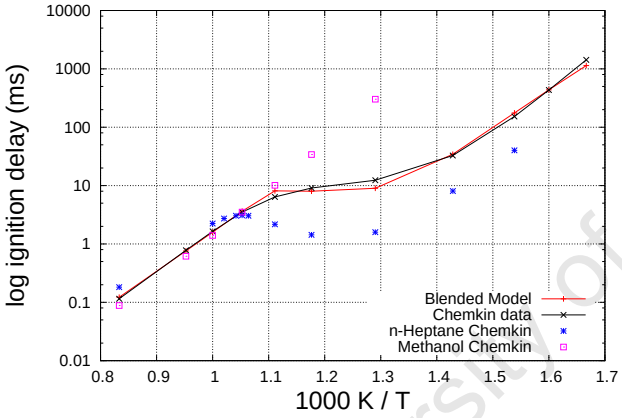

(a) Ignition delay diagram

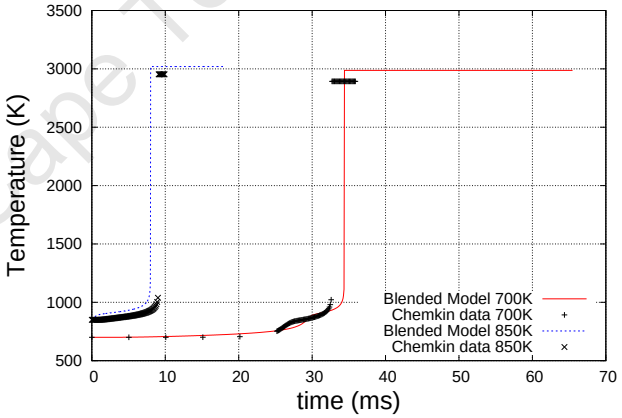

(b) Temperature-time profiles

Figure 5.27: Binary blend, by liquid volume 60% methanol and 40% n-heptane (84.5/15.5% mole)

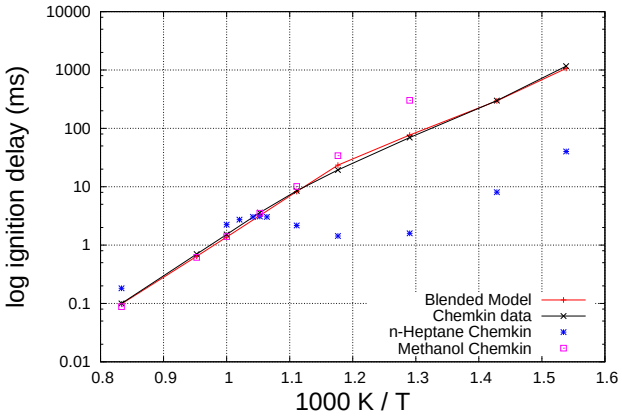

(a) Ignition delay diagram

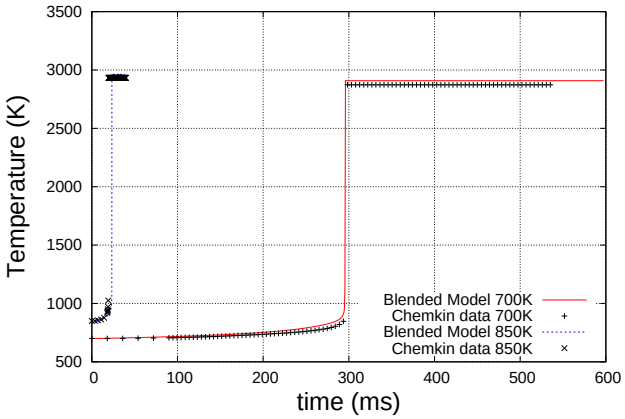

(b) Temperature-time profiles

Figure 5.28: Binary blend, by liquid volume 80% methanol and 20% n-heptane (93.5/6.5% mole)

Overall the ignition delay diagrams of the methanol-heptane blends are not very well predicted, especially as the methanol content increases. This can be attributed to the extreme NTC behaviour seen in the ignition delay behaviour of n-heptane in figure 5.1 compared to the non-existent low temperature kinetics of methanol in figure 5.11.

5.5 Ternary Blends

The model used to predict blends between i-octane and methanol is obtained from a combination of model C, model D and model E. A example of combining three models to obtain a ternary blended model is given in section 7.2 in Appendix .

The rate constants for the ternary blends were obtained without regression using only the binary interactions obtained from the binary mixtures.

The combustion of all the blends were simulated at 20 bar and at stoichiometric ratios with air. The ignition delay diagrams for pure n-heptane and i-octane are plotted as points of reference for each fuel blend.

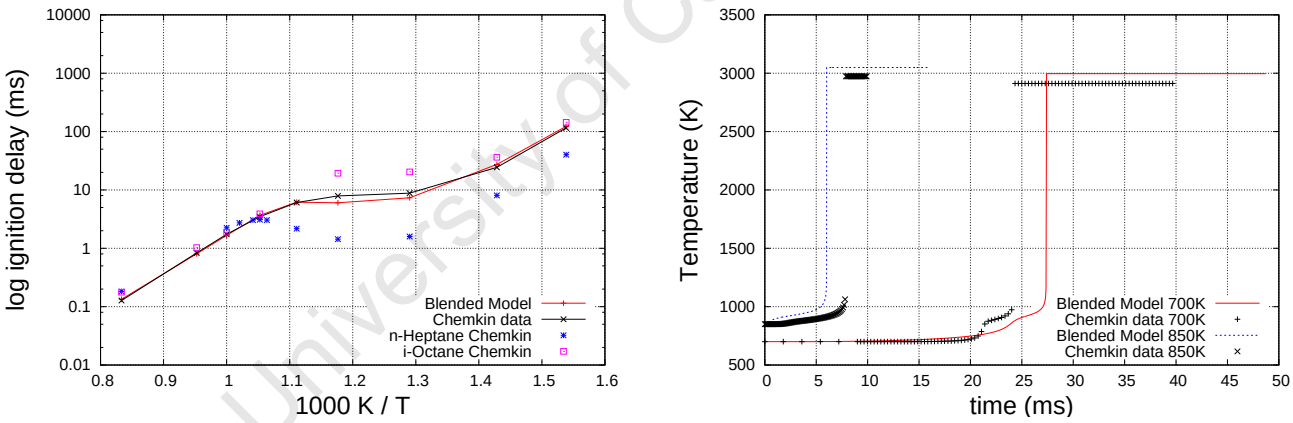

(a) Ignition delay diagram

(b) Temperature-time profiles

Figure 5.29: Ternary blend, by liquid volume 33% i-octane, 33% n-heptane, 34% methanol (16.3/18.3/65.4% mole)

Overall, the ignition delay prediction of the blend in figures 5.29a and 5.30a is good, except for the NTC region. The 2 stage ignition is also poorly predicted as seen in the temperature-time profiles in figures 5.29b and 5.30b. This highlights the dependence of an accurate prediction of the NTC region on the accurate prediction of the 2 stage ignition.

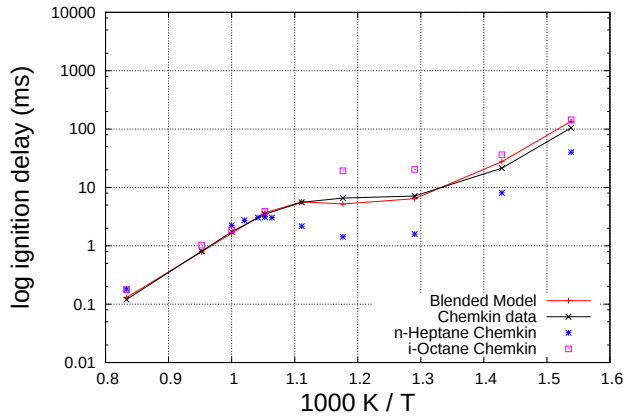

(a) Ignition delay diagram

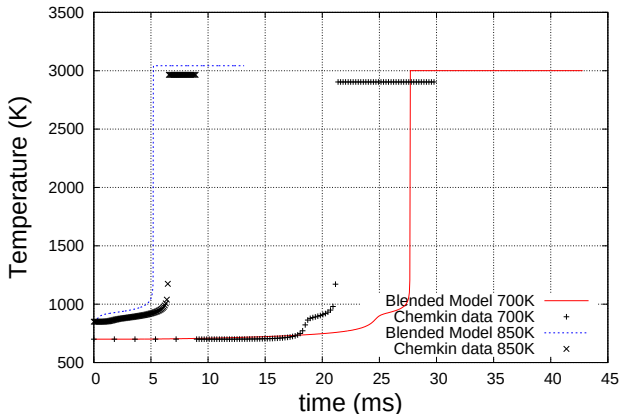

(b) Temperature-time profiles

Figure 5.30: Ternary blend, by liquid volume 10% i-octane, 45% n-heptane, 45% methanol (4.1/20.8/75.2% mole)

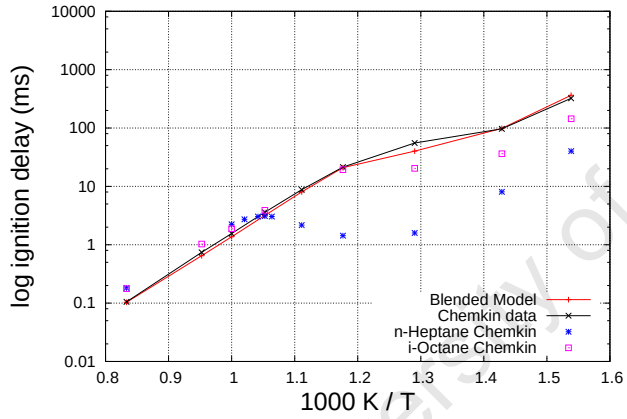

(a) Ignition delay diagram

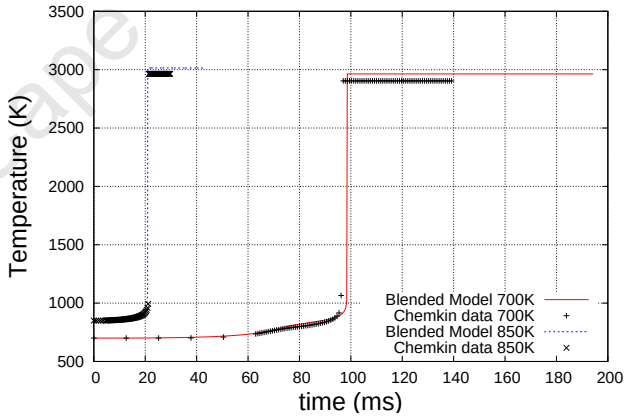

(b) Temperature-time profiles

Figure 5.31: Ternary blend, by liquid volume 45% i-octane, 10% n-heptane, 45% methanol (18.8/4.6/76.6% mole)

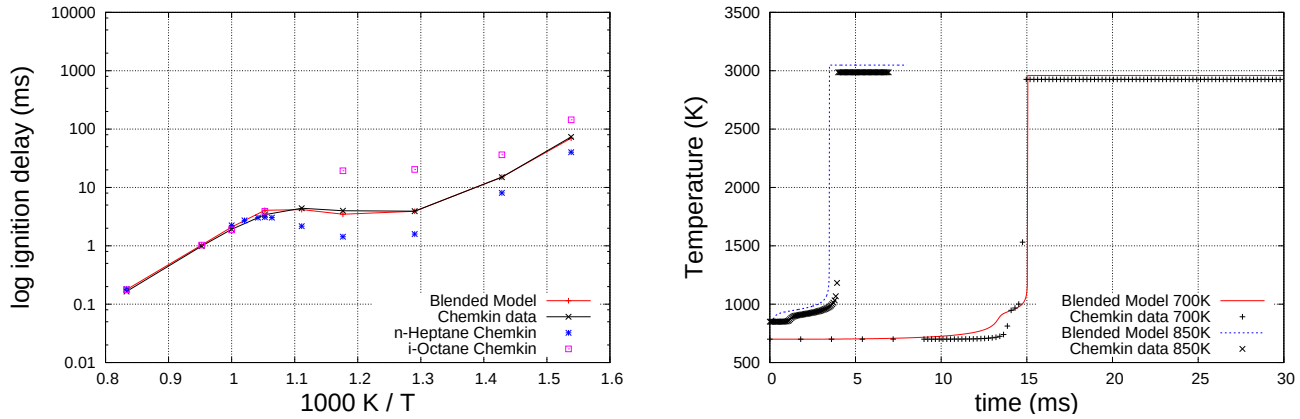

(a) Ignition delay diagram

(b) Temperature-time profiles

Figure 5.32: Ternary blend, by liquid volume 45% i-octane, 45% n-heptane, 10% methanol (33.3/37.1/29.9% mole)

Generally, the ignition delay diagrams of the ternary blends are accurately predicted, especially considering that the prediction involves no regression. The predictions are made using the mixing rules laid out in section 4.4 and the binary interaction parameters obtained from the binary blends.

5.6 Results Summary

5.6.1 Pure Fuels

Model C and model D, for n-heptane and i-octane respectively, predict the 'cool' flame shape and the magnitude of the 'cool' flame relatively well compared to the Schreiber model. However, the inability to predict shorter second ignition delays means that the location of the 'cool' flame ignition is inaccurate. The location of the 'cool' flame ignition is sacrificed to predict the correct final ignition delay which is well predicted by model C and model D. It is clear that a good 'cool' flame prediction is needed to correctly predict ignition delay in the NTC region. Therefore good estimates of the low temperature parameters require the regression of not only ignition delay data, but also temperature-time data.

Model E, for methanol, contains only high temperature kinetics so it predicts the ignition delay well.

5.6.2 Binary Blends

The blended models successfully predict the ignition delay of binary blends through the regression of binary interaction parameters. The regression of the binary interaction parameters is simpler

between fuels with similar ignition behaviour (n-heptane/i-octane).

5.6.3 Ternary Blends

Without regression the ignition delays for ternary blends are successfully predicted using the blended model and the binary interaction parameters.

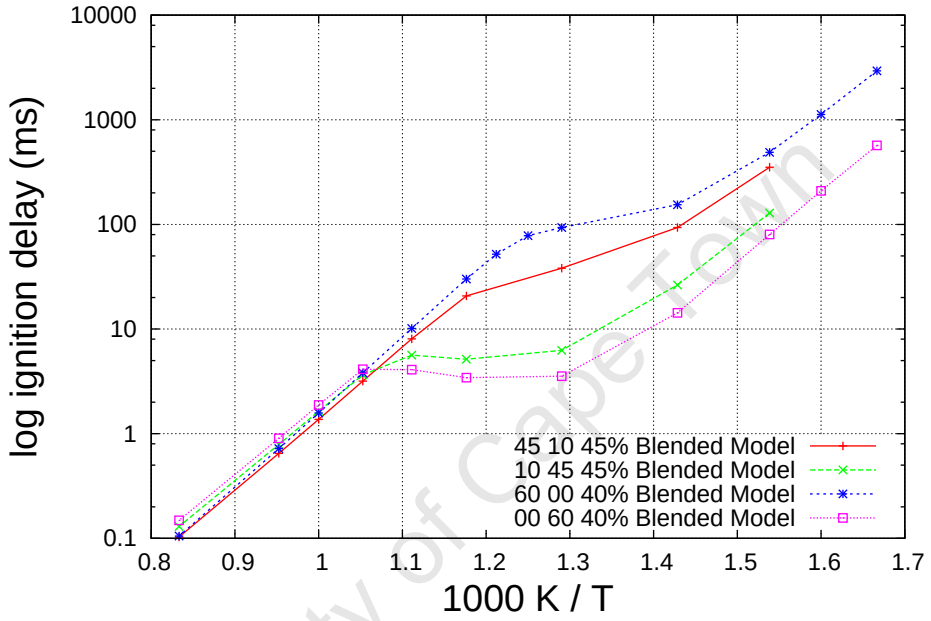

Figure 5.33: Similar alkane/methanol blends

Figure 5.33 compares the ignition delay diagrams of fuels blends with similar ratios of alkane fuels to methanol. It shows that one alkane cannot be used to represent another alkane or a blend of alkanes. However, the quantification of the %NTC behaviour associated with the alkane can be used to predict blends with similar ignition delay behaviour. The extent of NTC behaviour is quantified by Viljoen (2009) as %NTC. For n-heptane and i-octane their NTC behaviour is quantified as 90.47% NTC and 50.25% NTC respectively. The quantification of i-octane's NTC behaviour is not correct for the current system. From inspection of figure 5.34 the pure i-octane is closest to the 40% n-Heptane/60% methanol blend. If the %NTC of n-heptane is taken as 90.47%, then the NTC% of the 40% n-Heptane/60% methanol blend is 36.19% (refer to table 5.10). Therefore the NTC% of pure i-octane is closer to 40% rather than 50.25%.

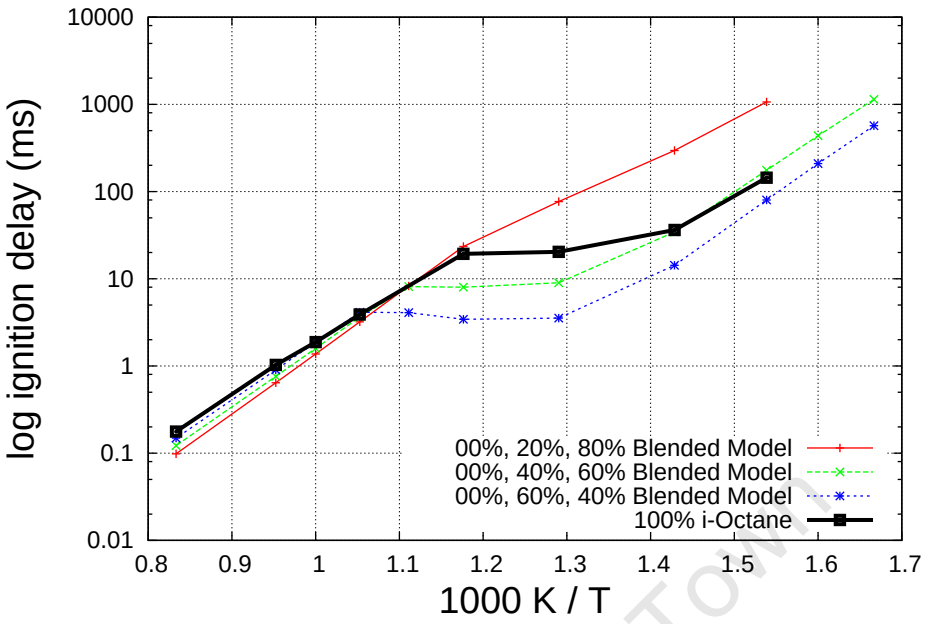

Figure 5.34: Similar alkane/methanol blends. Composition is given as i-octane, n-heptane and methanol respectively.

Table 5.10: Calculating %NTC associated with the blend

	i-Octane	n-Heptane	Methanol	Overall
% composition	0	20	80	100
% NTC	0	18.09	0	18.09
% composition	0	40	60	100
% NTC	0	36.19	0	36.19
% composition	0	60	40	100
% NTC	0	54.28	0	54.28

Using %NTC of 40% for i-octane the blends can be ranked by %NTC in table 5.11.

Table 5.11: Ranking of %NTC associated with the blends

	i-Octane	n-Heptane	Methanol	Overall %NTC
% Composition of Blend	40	0	60	16
% Composition of Blend	0	20	80	18
% Composition of Blend	60	0	40	24
% Composition of Blend	45	10	45	27
% Composition of Blend	80	20	0	32
% Composition of Blend	0	40	60	36
% Composition of Blend	33	33	34	43
% Composition of Blend	10	45	45	44
% Composition of Blend	80	20	0	50
% Composition of Blend	0	60	40	54
% Composition of Blend	45	45	10	58
% Composition of Blend	60	40	0	60
% Composition of Blend	40	60	0	70
% Composition of Blend	0	80	20	72
% Composition of Blend	20	80	0	80

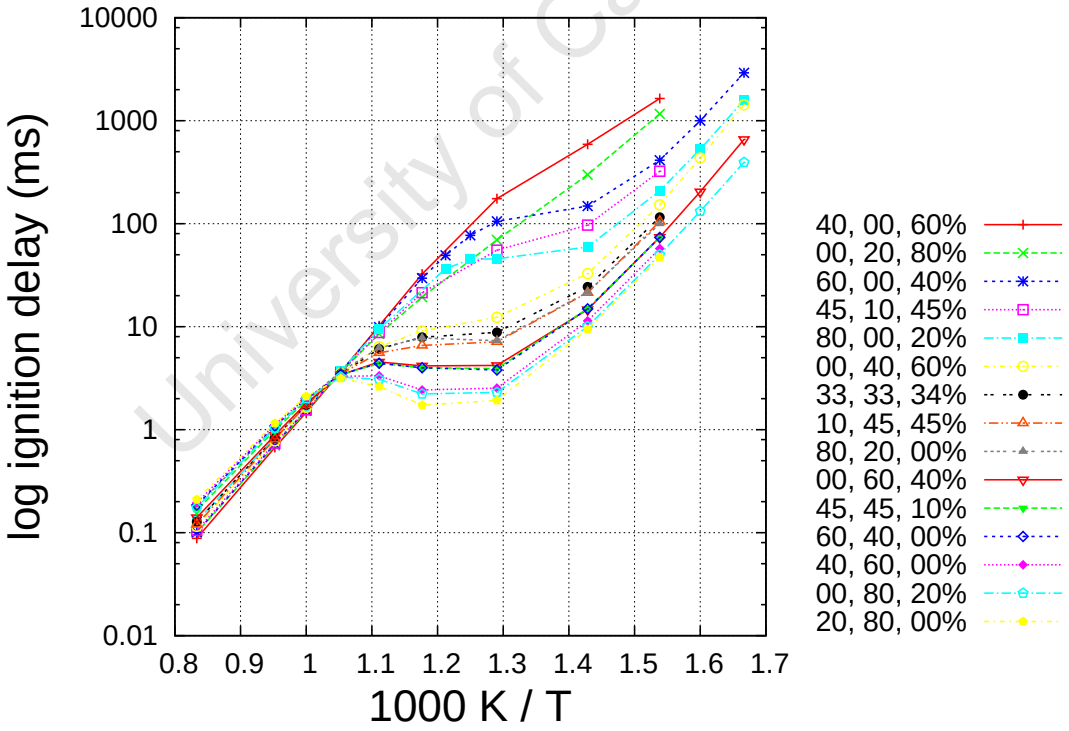

Figure 5.35: Ignition delay diagrams for i-octane/n-heptane/methanol blends. Composition percentages are given as i-octane, n-heptane and methanol respectively.

The ranking in table 5.11 is graphically represented in figure 5.35 where the NTC behaviour of the blends can be seen to increase as their %NTC increases.

Therefore blends with the same %NTC should have similar or identical ignition delay diagrams. Three blends with %NTC of 60% are shown in table 5.12 and their ignition delay diagrams are presented in figure 5.36. The three ignition delay diagrams show enough similarity for it to be concluded that %NTC can be used as a relevant factor for predicting ignition behaviour. Potentially, one hydrocarbon could be used to represent all the hydrocarbons from its hydrocarbon class, providing the %NTCs of the hydrocarbons are incorporated.

Table 5.12: %NTC of 60% for various blends

	i-Octane	n-Heptane	Methanol	Overall
% composition	60	40	0	100
% NTC	24	36	0	60
% composition	0	66	34	100
% NTC	0	60	0	60
% composition	46	46	8	100
% NTC	18	42	0	60

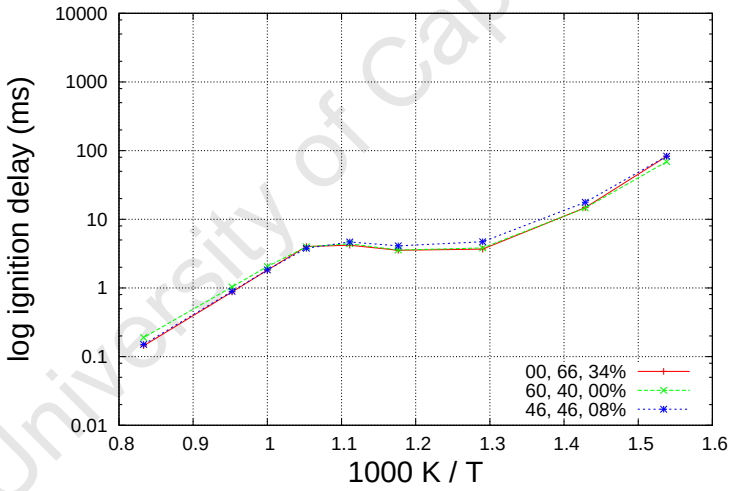

Figure 5.36: Ignition delay diagrams for various blends with %NTC of 60%. Composition is given as i-octane, n-heptane and methanol respectively.

Viljoen (2009) quantified the %NTC associated with compounds and used %NTC together with an empirical octane prediction model developed by Twu and Coon (1997) to predict the octane number of blends. Figure 5.36 suggests that %NTC could be used to predict the ignition delay diagrams of blends, possibly by incorporating the octane number. Conversely, the ignition delay diagram of a fuel could be used to estimate its %NTC and therefore its octane number.

5.7 Result's Error Summary

5.7.1 Pure Fuels

Table 5.13: Error analysis of pure fuels based on ignition delay diagrams

Blend	Standard Error at 20 bar	Standard Error at 30 bar	Standard Error at 40 bar
	$s = \sqrt{\frac{S(\theta)}{N}}$	$s = \sqrt{\frac{S(\theta)}{N}}$	$s = \sqrt{\frac{S(\theta)}{N}}$
n-heptane	0.062	0.068	0.072
i-octane	0.080	0.09	0.19
methanol	0.11	0.04	0.13

The pressure constants were regressed for ignition delay of n-heptane and then used unchanged for the i-octane and methanol. Visually the the ignition delay diagrams of methanol and i-octane are well predicted at varying pressures. However, the standard errors at the various pressures indicate that the pressure constants are not accurate for all the fuels.

5.7.2 Binary Blends

Table 5.14: Error analysis of fuel blends based on ignition delay diagrams at 20 bar

Blend	Standard Error
	$s = \sqrt{\frac{S(\theta)}{N}}$
n-heptane/i-octane	0.073
i-octane/methanol	0.078
n-heptane/methanol	0.112

The NTC behaviour is what makes predicting the ignition delay of the blends complicated. The NTC behaviour of n-heptane and i-octane is quantified as 90.47% NTC and 50.25% NTC respectively (Viljoen, 2009). Methanol with no NTC behaviour would have 0% NTC. These percentages help explain the accuracy of the blend predictions. The n-heptane/i-octane is the most accurate as both fuels have significant NTC behaviour. The accuracy of the i-octane/methanol blend is more accurate than the n-heptane/methanol because the difference in %NTC is far smaller for the i-octane/methanol blend. The inferior fit of the methanol/n-heptane blends can be seen visually in section 5.4 as well as by comparing the standard errors in table 5.14. The standard errors of the individual n-heptane/methanol blends are presented in table 5.15. Figure 5.15 shows that it is the blends with similar liquid volumes of each pure fuel which have the least accurate ignition delay predictions. Figure 5.26a and figure 5.27a show that it is the NTC region which is the least

accurately predicted, confirming the conclusion that it is the extreme NTC behaviour of n-heptane causing the complications.

Table 5.15: Error analysis of n-heptane/methanol fuel blends based on ignition delay diagrams at 20 bar

Blend	Standard Error
Percentage by volume	$s = \sqrt{\frac{S(\theta)}{N}}$
80 % n-heptane / 20% methanol	0.076
60 % n-heptane / 40% methanol	0.115
40 % n-heptane / 60% methanol	0.145
20 % n-heptane / 80% methanol	0.100

5.7.3 Ternary Blends

The ternary blends are poorly predicted for certain blends and this can be attributed to the poor prediction of the binary blends interactions which make up the ternary blends. Specifically it is the poor prediction of the n-heptane/methanol blend which results in the relatively poor prediction of the ternary blends. This is verified by the error associated with the individual ternary blends in table 5.16, where it can be seen that the highest error is associated with blend number 2, where the n-heptane/methanol binary interaction is the most significant.

Table 5.16: Error analysis of individual ternary fuel blends based on ignition delay diagrams at 20 bar

Blend number	Blend	Objective function
	Percentage by volume	$s = \sqrt{\frac{S(\theta)}{N}}$
1	33% i-octane, 33% n-heptane, 34% methanol	0.123
2	10% i-octane, 45% n-heptane, 45% methanol	0.141
3	45% i-octane, 10% n-heptane, 45% methanol	0.133
4	45% i-octane, 45% n-heptane, 10% methanol	0.103
	Average for ternary blends	0.126

to

Chapter 6

Conclusions

6.1 Outcomes

- The ignition delays of the pure fuels were accurately predicted. The temperature-time profiles in the instances of two stage ignition are relatively inaccurate because the 'cool' flame is predicted too early and the second ignition delay is too long. The temperature profiles are however an improvement on the temperature profiles predicted by the Schreiber model, particularly in terms of the slow temperature rise during the ignition delay and the sharp temperature rise during ignition. These were two of the main phenomena identified as needing improvement.
- Overall the ignition delays of binary fuel blends were accurately predicted using binary interactions. However, when modelling the blends between methanol and n-heptane, where one fuel has extreme NTC behaviour and the other fuel has no NTC behaviour, the predictions were less accurate.
- It is shown that by using binary interactions a ternary mixture could be accurately predicted without any further regression or parameter fitting. The accuracy of the ternary mixture predictions are dependent on the accuracy of the binary interaction parameters.
- The proposed model with the associated binary interaction functions is a theoretically viable method for modelling the combustion of fuel surrogates and can therefore be used in CFD work.
- %NTC of a hydrocarbon blend could be used to predict the shape of the blend's ignition delay diagram.
- Using a genetic algorithm was found to be a satisfactory method for solving a highly nonlinear and complex system where the parameters are often highly correlated. It was however a very

computationally expensive method.

- The final temperatures reached in the temperature-time profiles were not consistent with those obtained by CHEMKIN. This is either due to incorrect assumptions made in finding the temperature dependent heat capacity or possible inaccuracies in the detailed kinetics used by CHEMKIN.

6.2 Model Improvements

- There is a deficiency in the proposed model which does not accelerate the high temperature oxidation if the cool flame has taken place. There needs to be some chemical interaction between the cool flame and the high temperature oxidation rather than just thermal interaction. The effects of third body efficiency was added as an attempt to provide the chemical interaction between the low temperature and the high temperature oxidation. Its effects were not pronounced enough to capture the behaviour required. Yates and Viljoen (2008) used an 'X' scaling factor to account for the chemical influence of the 'cool' flame on the high temperature oxidation, which is a possible solution. The 'X' factor is however not based on any reaction or theory.

- The model needs to be validated and adapted for extended pressure ranges and various air fuel ratios to make it more comprehensive.

- The rate constants and binary interaction parameters for further pure fuels and binary combinations need to be obtained for further validation of the method used in this study. Detailed mechanisms do not all agree, so a new mechanism which is valid for all the fuels required would need to be used as the basis for fitting the parameters. Currently the mechanism published by Mehl et al. (2009) is suitable as it is valid for the PRFs, butane, 1-hexene and toluene. The mechanism is therefore valid for many of the gasoline surrogates proposed in the literature.

- If the model is to be used in CFD work, the method of finding a global heat capacity for the system will have to be changed. In CFD flow reactors, properties are needed for each species to obtain the temperature and velocity fields. Therefore, each species (F, I, P, X) will need to have their own heat capacity and it will be necessary to regress for these values.

Bibliography

Agosta, A., Cernansky, N. P., Miller, D. L., Faravelli, T., Ranzi, E., 2004. Reference components of jet fuels: kinetic modeling and experimental results. Experimental Thermal and Fluid Science 28 (7), 701 – 708, 3rd Mediterranean Combustion Symposium.

Andrae, J., 2008. Development of a detailed kinetic model for gasoline surrogate fuels. Fuel 87 (10-11), 2013 – 2022.

Ashman, P. J., Haynes, B. S., 1998. Rate coefficient of H + O2 + M -> HO2 + M (M=H2O, N2, AR, CO2). 27th Symposium (International) on Combustion 27, 185 – 191.

Battin-Leclerc, F., 2008. Detailed chemical kinetic models for the low-temperature combustion of hydrocarbons with application to gasoline and diesel fuel surrogates. Progress in Energy and Combustion Science 34 (4), 440 – 498.

Benson, S., 1976. Thermochemical Kinetics. New York: Wiley.

Brennan, K., Campbell, S., Petzold, L., 1989. Numerical solution of initial-value problems in diffrential-algebraic equations. North Holland.

Caracotsios, M., Stewart, W. E., 1995. Sensitivity analysis of initial-boundary-value problems with mixed PDEs and algebraic equations: Applications to chemical and biochemical systems. Computers & Chemical Engineering 19 (9), 1019 – 1030.

Carroll, D., 1996. Chemical laser modeling with genetic algorithms. AIAA Journal 34.

Chevalier, C., Pitz, W., Warnatz, J., Westbrook, C. K., Melenk, H., 1992. Hydrocarbon ignition : automatic generation of reaction mechanisms and applications to modelling of engine knock. In: 24th Symposium (International) on Combustion. The Combustion Institute, Pittsburgh, USA, pp. 93–101.

Cox, R. A., Cole, J. A., 1985. Chemical aspects of the autoignition of hydrocabon-air mixtures. Combustion and Flame 60, 109–123.

Curran, H., Gaffuri, P., Pitz, W. J., Westbrook, C. K., 2002. A comprehensive modeling study of iso-octane oxidation. Combustion and Flame 129 (3), 253–280.

Curran, H. J., Gaffuri, P., Pitz, W. J., Westbrook, C. K., 1998. A comprehensive modelling study of h-heptane oxidation. Combustion and Flame 114, 149–177.

Davis, L. (Ed.), 1996. Handbook of Genetic Algorithms. International Thomson Computer Press.

Elliott, L., Ingham, D., Kyne, A., Mera, N., Pourkashanian, M., Wilson, C., 2005. The use of ignition delay time in genetic algorithms optimisation of chemical kinetics reaction mechanisms. Engineering Applications of Artificial Intelligence 18 (7), 825 – 831.

Elliott, L., Ingham, D. B., Kyne, A. G., Mera, N. S., Pourkashanian, M., Wilson, C. W., 2004. Genetic algorithms for optimisation of chemical kinetics reaction mechanisms. Progress in Energy and Combustion Science 30 (3), 297 – 328.

Fikri, M., Herzler, J., Starke, R., Schulz, C., Roth, P., Kalghatgi, G., 2008. Autoignition of gasoline surrogates mixtures at intermediate temperatures and high pressures. Combustion and Flame 152 (1-2), 276 – 281.

Frenklach, M., Wang, H., 1991. Detailed reduction of reaction mechanisms for flame modelling. Combustion and Flame 87, 365–370.

Gauthier, B., Davidson, D., Hanson, R., 2004. Shock tube determination of ignition delay times in full-blend and surrogate fuel mixtures. Combustion and Flame 139 (4), 300 – 311.

Griffiths, J. F., 1993. Kinetic fundamentals of alkane autoignition at low temperatures. Combustion and Flame 93, 202–206.

Griffiths, J. F., 1995. Reduced kinetic models and their application to practical combustion systems. Prog. Energy Combust. Sci. 21, 25 – 107.

Hughes, M., 2009. Optimisation of complex distillation column systems using rigorous models. Ph.D. thesis, University of Cape Town.

Kolaitis, D. I., Founti, M. A., 2009. On the assumption of using n-heptane as a surrogate fuel for the description of the cool flame oxidation of diesel oil. Proceedings of the Combustion Institute 32 (2), 3197 – 3205.

Levenspiel, O., 1999. Chemical Reaction Engineering. John Wiley & Sons.

Lu, P., Binita, B., Barton, P. I., Green, W. H., 2003. Reduced models for adaptive chemistry simulation of reacting flows. In: Bathe, K. (Ed.), Computational Fluid and Solid Mechanics 2003. Elsevier Science Ltd, Oxford, pp. 1422 – 1425.

Lu, T., Law, C. K., 2009. Toward accommodating realistic fuel chemistry in large-scale computations. Progress in Energy and Combustion Science 35 (2), 192 – 215.

Machrafi, H., Cavadias, S., 2008. Three-stage autoignition of gasoline in an HCCI engine: An experimental and chemical kinetic modeling investigation. Combustion and Flame 155 (4), 557 – 570.

Mehl, M., Curran, H. J., Pitz, W. J., Westbrook, C. K., 2009. Detailed kinetic modeling of gasoline surrogate mixtures. In: 6th U.S. National Combustion Meeting.

Minetti, R., Carlier, M., Ribaucour, M., Therssen, E., Sochet, L. R., 1995. A rapid compression machine investigation of oxidation and auto-ignition of n-heptane : measurements and modelling. Combustion and Flame (102), 298–309.

Muller, C., Michel, V., Scacchi, G., Come, G., 1995. A computer program for the evaluation of thermochemical data of molecules and free radicals in the gas phase. J Chem Phys 92.

Muller, U. C., Peters, N., Linan, A., 1992. Global kinetics for n-heptane ignition at high pressures. In: 24th Symposium (International) on Combustion. The Combustion Institute, Pittsburgh, USA, pp. 777–784.

Petzold, L., 1982. A description of DASSL: a differential/algebraic solver. Sandia Tech. Rep., 82 – 8637.

Pitz, W. J., Cernansky, N. P., Dryer, F. L., Egolfopoulos, F. N., Farrell, J. T., Friend, D. G., Pitsch, H., 2007. Development of an experimental database and kinetic models for surrogate gasoline fuels. SAE Paper.

Sandler, S. I., 2006. Chemical, Biochemical, and Engineering Thermodynamics, 4th Edition. John Wiley & Sons.

Schreiber, M., Sakak, A. S., Lingens, A., Griffiths, J. F., 1994. A reduced thermokinetic model for the autoignition of fuels with variable octane ratings. In: 25th Symposium (International) on Combustion. The combustion institute, Pittsburgh, USA, pp. 933–940.

Stewart, W. E., Caracotsios, M., SÃžrensen, J. P., 1992. Parameter estimation from multiresponse data. AIChE Journal 38, 641–650.

Tanaka, S., Ayala, F., Keck, J. C., Heywood, J. B., 2003. Two-stage ignition in HCCI combustion and HCCI control by fuels and additives. Combustion and Flame 132 (1-2), 219 – 239.

Turns, S., 2000. An Introduction to Combustion: Concepts and Applications. McGraw-hill.

Twu, C., Coon, J., 1997. Estimate octane numbers using an enhanced method. Hydrocarbon Processing 75, 65–68.

Vanhove, G., Petit, G., Minetti, R., 2006. Experimental study of the kinetic interactions in the low-temperature autoignition of hydrocarbon binary mixtures and a surrogate fuel. Combustion and Flame 145 (3), 521 – 532.

Viljoen, C., 2009. Assessment of disparate strategies for octane prediction. Ph.D. thesis, University of Cape Town.

Viljoen, C., Yates, A., Swarts, A., Balfour, G. Moller, K., 2005. An investigation of the ignition delay character of different fuel components and an assessment of various autoignition modelling approaches. SAE.

Violi, A., Yan, S., Eddings, E., Sarofim, A., Granata, S., Faravelli, T., Ranzi, E., 2002. Experimental formulation and kinetic model for JP-8 surrogate mixtures. Combustion Science and Technology 174 ((11-12)), 399–417.

Warnatz, J., Maas, U., Dibble, R., 2001. Combustion : Physical and Chemical Fundamentals, Modeling and Simulation, Experiments, Pollutant Formation. Springer Verlag.

Yates, A., Bell, A., Swarts, A., 2010. Insights relating to the autoignition characteristics of alcohol fuels. Fuel 89, 83–89.

Yates, A., Viljoen, C., 2008. An improved empirical model for describing autoignition. SAE 2008-01-1629.

Zheng, J., Miller, D., Cernansky, N., 2004. A global reaction model for the HCCI combustion process. SAE.

Chapter 7

Appendix A

7.1 Binary Blend Example

As an example of how a blended model and its blend reaction constants are calculated, the constants have been calculated for the binary blend of 60% i-octane and 40% methanol (by liquid volume).

Firstly, the fuel composition needs to be converted into a molar basis which is 26.9% i-octane and 73.1% methanol. Therefore the basic oxidation reaction upon which the model is based is:

$$fuel + 4.27O_2 \Rightarrow 2.88CO_2 + 3.51H_2O \tag{7.1}$$

The stoichiometric ratios in equation 7.2 are obtained using the basic oxidation reactions of methanol (equation 4.16) and i-octane (equation 4.15) together with the fuel composition. The O_2 multiplier is for example found in the following way using the molar composition:

$$4.27 = 0.269 * 12.5 + 0.731 * 1.5$$

7.1.1 Blended Binary Model

Table 7.1: Model G, adapted from model D and model E for the binary blend of 60% i-octane and 40% methanol (by liquid volume)

High Temperature Kinetics		
Reaction name	Reaction	Reaction Rates
G1	$F_T \rightarrow X$	$R_1 = k_1 M[F_T](\frac{p}{p_0})^{-1.0}$
G2	$X + 4.27O_2 \rightarrow P$	$R_2 = k_2[X][O_2]$
Low Temperature Kinetics		
Reaction name	Reaction	Reaction Rates
G3	$F_L + 2O_2 \rightarrow I$	$R_3 = k_3[F_L][O_2](\frac{p}{p_0})^{-0.5}$
G4+	$I + F_L + 2O_2 \rightarrow 2I$	$R_{4+} = k_{4+}[I][F_L][O_2](\frac{p}{p_0})^{-1.4}$
G4-	$2I \rightarrow I + F_L + 2O_2$	$R_{4-} = k_{4-}[I]$
G5	$I + 2.27O_2 \rightarrow P$	$R_5 = k_5[O_2][I]^2$

7.1.2 Blended Binary Rate Constants for High Temperature Kinetics

The model parameters are calculated using the proposed mixing rules discussed in Section 4.4.2. For reaction G1 the parameters A_{mix}, Ea_{mix} and $\triangle H_{rxn,mix}$ are calculated as an example in the high temperature kinetics. For A_{mix} equation 4.35 is used.

$$ln(A_{1,mix}) = \sum_{i=1}^{C} x_i ln(A_{1,i}) + \sum_{i=1}^{C-1} \sum_{j=i+1}^{C} f_A(x_i, x_j)$$

where

$$f_A(x_i, x_j) = x_i^{n_{1,ij}} x_j^{2-n_{1,ij}} w_{1,ij}$$

For the i-octane/methanol blend, the interaction parameters for the pre-exponent rate constant for reaction 1 are given in table 7.2.

Table 7.2: Interaction parameters for reaction 1 in the binary blend between i-octane and methanol

	A_1	
Reaction No.	n	w
1	0.89	-0.90

$$f_A(x_{meth}, x_{i-oct}) = 0.731^{0.89} * 0.269^{(2-0.89)} * (-0.9) = -0.155$$

$$ln(A_{1,mix}) = 0.269 * ln(7.5 \times 10^5) + 0.731 * ln(2.43 \times 10^7) - 0.155 = 15.91$$

$$A_{1,mix} = e^{15.91} = 8.2 \times 10^6$$

For $Ea_{1,mix}$ equation 4.36 is used.

$$Ea_{1,mix} = \sum_{i=1}^{C} x_i (Ea_{1,i}) + \sum_{i=1}^{C-1} \sum_{j=i+1}^{C} f_{1,Ea}(x_i, x_j)$$

where

$$f_{Ea,1}(x_i, x_j) = x_i^{ne_{1,ij}} x_j^{2-ne_{1,ij}} we_{1,ij}$$

For the i-octane/methanol blend, the interaction parameters for the activation energy for reaction 1 are given in table 7.3.

Table 7.3: Interaction parameters for reaction 1 in the binary blend between i-octane and methanol

	$\frac{Ea_1}{R}$	
Reaction No.	ne	we
1	1.50	-690.00

$$f_{Ea,1}(x_{meth}, x_{i-oct}) = 0.731^{1.5} * 0.269^{(2-1.5)} * (-690.0) = -223.7$$

$$Ea_{1,mix} = 0.269 * (17.7 \times 10^3) + 0.731 * (21.1 \times 10^3) - 223.7 = 20.0 \times 10^3$$

For $\triangle H_{rxn,mix}$ equation 4.37 is used.

$$\triangle H_{rxn,1,mix} = 0.269 * (-709.9) + 0.731 * (-60.0) = -234.4$$

7.1.3 Blended Binary Rate Constants for Low Temperature Kinetics

Since the methanol does not have low temperature kinetics the parameters for the low temperature kinetics use the special case mixing laws as discussed in Section 4.4.3. For reaction G3 the parameters A_{mix}, Ea_{mix} and $\triangle H_{rxn,mix}$ are calculated as an example. To calculate $A_{3,mix}$ equation 4.45 is used together with the binary interaction term, equation 4.43.

$$ln(A_{3,mix}) = y_i ln(A_{3,i}) + fSP_A(x_i, y_j)$$

where

$$fSP_{A,3}(x_i, y_j) = y_j x_i^{n_{3,ij}} w_{3,ij}$$

For the i-octane/methanol blend, the interaction parameters for the pre-exponent rate constant for reaction 3 are given in table 7.4.

Table 7.4: Interaction parameters for reaction 3 in the binary blend between i-octane and methanol

	A_3	
Reaction No.	n	w
3	5.90	-3.60

$$fSP_{A,3}(x_{meth}, y_{i-oct}) = 1.0 * 0.731^{5.90} * (-3.60) = -0.567$$

$$ln(A_{3,mix}) = 1.0 * ln(1.0 \times 10^5) - 0.567 = 10.95$$

$$A_{3,mix} = e^{10.95} = 5.67 \times 10^4$$

For Ea_{mix} equation 4.46 is used.

$$Ea_{3,mix} = y_j(Ea_{3,,j}) + fSP_{Ea}(x_i, y_j)$$

where the binary function is given by equation 4.44

$$fSP_{Ea,3}(x_i, y_j) = y_j x_i^{ne_{3,ij}} we_{3,ij}$$

For the i-octane/methanol blend, the interaction parameters for the activation energy for reaction 3 are given in table 7.5.

Table 7.5: Interaction parameters for reaction 3 in the binary blend between i-octane and methanol

	$\frac{Ea_3}{R}$	
Reaction No.	ne	we
3	3.00	870.00

$$f_{Ea}(x_{meth}, y_{i-oct}) = 1.0 * 0.731^{3.0} * (870.0) = 337.0$$

$$Ea_{3,mix} = 1.0 * (10.7 \times 10^3) + 337.0 = 11.0 \times 10^3$$

To calculate$\triangle H_{rxn,mix}$ equation 4.40 is used.

$$\triangle H_{3,rxn,mix} = 1.0 * (20.0) = 20.0$$

When applied to all the rate constants, the complete set of rate constants are obtained below.

Table 7.6: Parameters for i-octane/methanol blend used in binary blended model G

Reaction Name	$\triangle H_{rxn}$	A	$\frac{Ea}{R}$	Pressure constant
	kJ/mol	Reaction specific	K	
G1	-234.4	8.15×10^6	20.0×10^3	-1.00
G2	1840.0	6.15×10^6	1.04×10^3	
G3	20.0	5.71×10^4	11.0×10^3	-0.5
G4+	20.0	3.24×10^{13}	25.6×10^3	-1.4
G4-	-20.0	2.13×10^{23}	37.7×10^3	
G5	4500.0	6.00×10^{15}	26.0×10^3	

Air is added to the system to obtain a stoichiometric ratio of fuel to air. This means that the initial system composition on a molar basis is 5.5% fuel, 20.0% oxygen and 74.5% nitrogen.

7.2 Ternary Blend Example

The blended model and its blend reaction constants are calculated for the ternary blend of 33% i-octane, 33% n-heptane and 34% methanol (by liquid volume).

Firstly, the fuel composition needs to be converted to a molar basis, which is 16.3%, 18.3% and 65.4% for i-octane, n-heptane and methanol respectively. Therefore the basic oxidation reaction upon which the model is based is:

$$fuel + 4.87O_2 \Rightarrow 3.24CO_2 + 3.91H_2O \tag{7.2}$$

The stoichiometric ratios in equation 7.2 are obtained using the basic oxidation reactions of methanol (equation 4.16), n-heptane (equation 4.14) and i-octane (equation 4.15) together with the fuel composition. The O_2 multiplier is for example found in the following way using the molar composition:

$$4.87 = 0.163 * 12.5 + 0.183 * 11.5 + 0.654 * 1.5$$

7.2.1 Blended Ternary Model

Table 7.7: Model F, adapted from models C, D and E for the ternary blend of of 33% i-octane, 33% n-heptane and 34% methanol (by liquid volume)

High Temperature Kinetics		
Reaction name	Reaction	Reaction Rates
F1	$F_T \rightarrow X$	$R_1 = k_1 M[F_T](\frac{p}{p_0})^{-1.0}$
F2	$X + 4.87O_2 \rightarrow P$	$R_2 = k_2[X][O_2]$
Low Temperature Kinetics		
Reaction name	Reaction	Reaction Rates
F3	$F_L + 2O_2 \rightarrow I$	$R_3 = k_3[F_L][O_2](\frac{p}{p_0})^{-0.5}$
F4+	$I + F_L + 2O_2 \rightarrow 2I$	$R_{4+} = k_{4+}[I][F_L][O_2](\frac{p}{p_0})^{-1.4}$
F4-	$2I \rightarrow I + F_L + 2O_2$	$R_{4-} = k_{4-}[I]$
F5	$I + 2.87O_2 \rightarrow P$	$R_5 = k_5[O_2][I]^2$

7.2.2 Blended Binary Rate Constants for High Temperature Kinetics

The model parameters are calculated using the proposed mixing rules discussed in Section 4.4.2. For reaction F1 the parameters A_{mix}, Ea_{mix} and $\triangle H_{rxn,mix}$ are calculated as follows. For A_{mix} equation 4.35 is used.

$$ln(A_{1,mix}) = \sum_{i=1}^{C} x_i ln(A_{1,i}) + \sum_{i=1}^{C-1} \sum_{j=i+1}^{C} f_A(x_i, x_j)$$

where

$$f_A(x_i, x_j) = x_i^{n_{1,ij}} x_j^{2-n_{1,ij}} w_{1,ij}$$

For the binary blends, the interaction parameters for the pre-exponent rate constant for reaction 1 are given in table 7.8.

Table 7.8: Interaction parameters for pre-exponent rate constant A_i in reaction 1

	i-octane/n-heptane		i-octane/methanol		n-heptane/methanol	
Reaction No.	n	w	n	w	n	w
1	1.39	-0.41	0.89	-0.90	1.60	-4.40

$$\sum_{i=1}^{C-1}\sum_{j=i+1}^{C} f_A(x_i,x_j) = 0.183^{1.39} * 0.163^{(2-1.39)} * (-0.41) + 0.654^{0.89} * 0.163^{(2-0.89)} * (-0.9)$$

$$+0.654^{1.6} * 0.163^{(2-1.6)} * (-4.4) = 0.08$$

$$ln(A_{1,mix}) = 0.163 * ln(7.5 \times 10^5) + 0.183 * ln(1.69 \times 10^6) + 0.654 * ln(2.43 \times 10^7) - 0.08 = 14.77$$

$$A_{1,mix} = e^{14.77} = 2.6 \times 10^6$$

For Ea_{mix} equation 4.36 is used.

$$Ea_{1,mix} = \sum_{i=1}^{C} x_i(Ea_{1,i}) + \sum_{i=1}^{C-1}\sum_{j=i+1}^{C} f_{Ea}(x_i,x_j)$$

where

$$f_{Ea}(x_i,x_j) = x_i^{ne_{1,ij}} x_j^{2-ne_{1,ij}} we_{1,ij}$$

For the binary blends, the interaction parameters for the activation energy for reaction 1 are given in table 7.9.

Table 7.9: Interaction parameters for pre-exponent rate constant Ea_i in reaction 1

	i-octane/n-heptane		i-octane/methanol		n-heptane/methanol	
Reaction No.	ne	we	ne	we	ne	we
1	1.0	0.0	1.50	-690.00	1.70	-4000.00

$$\sum_{i=1}^{C-1}\sum_{j=i+1}^{C} f_{Ea,1}(x_i,x_j) = 0.183^{1.0} * 0.163^{(2-1.0)} * (0.0) + 0.654^{1.5} * 0.163^{(2-1.5)} * (-690) +$$

$$0.654^{1.7} * 0.163^{(2-1.7)} * (-4000) = -142.2$$

$$Ea_{1,mix} = 0.163 * 17.7 \times 10^3 + 0.183 * 18.7 \times 10^3 + 0.654 * 21.1 \times 10^3 - 142.2 = 18.9 \times 10^3$$

For $\triangle H_{rxn,1,mix}$ equation 4.37 is used.

$$\triangle H_{rxn,1,mix} = 0.163 * (-709.9) + 0.183 * (-709.9) + 0.654 * (-60.0) = -284.5$$

7.2.3 Blended Binary Rate Constants for Low Temperature Kinetics

Since the methanol does not have low temperature kinetics, the parameters for the low temperature kinetics use the special case mixing laws as discussed in Section 4.4.3. For reaction F3 the parameters A_{mix}, Ea_{mix} and $\triangle H_{rxn,mix}$ are calculated as an example. To calculate $A_{3,mix}$ equation 4.45 is used with the binary interaction term, equation 4.43, because methanol does not have low temperature kinetics.

$$ln(A_{3,mix}) = \sum_{i=1}^{C_L} y_i ln(A_{3,i}) + \sum_{i=1}^{C_L} \sum_{j=i+1}^{C} \begin{cases} if\ fuel\ j\ has\ low\ temperature\ kinetics & f_{3,A}(y_i, y_j) \\ else & fSP_{3,A}(y_i, x_j) \end{cases}$$

where

$$fSP_{A,3}(y_i, x_j) = y_i x_j^{n_{3,ij}} w_{3,ij}$$

and

$$f_{A,3}(y_i, y_j) = y_i^{n_{3,ij}} y_j^{2-n_{3,ij}} w_{3,ij}$$

For the binary blends, the interaction parameters for the pre-exponent rate constant for reaction 3 are given in table 7.10.

Table 7.10: Interaction parameters for pre-exponent rate constant A_i in reaction 3

	i-octane/n-heptane		i-octane/methanol		n-heptane/methanol	
Reaction No.	n	w	n	w	n	w
3	0.618	10.4	5.90	-3.60	23.00	-1.60

y_j is calculated for each component of the fuel:

$$y_{i-oct} = \frac{0.163}{0.183 + 0.163} = 0.47$$

$$y_{n-hept} = \frac{0.183}{0.183 + 0.163} = 0.53$$

$$f_{A,3}(y_{n-hept}, y_{i-oct}) = 0.53^{0.68} * 0.47^{(2-0.68)} * (8.64) = 2.15$$

$$fSP_{A,3}(x_{meth}, y_{i-oct}) = 0.47 * 0.654^{5.90} * (-3.60) = -0.140$$

$$fSP_{A,3}(x_{meth}, y_{n-hept}) = 0.53 * 0.654^{23.0} * (-1.60) = -4.40$$

$$ln(A_{3,mix}) = 0.47 * ln(1.0 \times 10^5) + 0.53 * ln(4.78 \times 10^6) + 2.15 - 0.14 - 4.40 = 14.34$$

$$A_{3,mix} = e^{14.34} = 1.7 \times 10^6$$

For $Ea_{3,mix}$ equation 4.36 is used.

$$Ea_{3,mix} = \sum_{i=1}^{C_L} y_i(Ea_{3,i}) + \sum_{i=1}^{C_L}\sum_{j=i+1}^{C} \begin{cases} if\ fuel\ i\ has\ low\ temperature\ kinetics & f_{Ea,3}(y_i, y_j) \\ else & fSP_{Ea,3}(x_i, y_j) \end{cases}$$

where

$$fSP_{Ea,3}(x_i, y_j) = y_j x_i^{ne_{3,ij}} we_{3,ij}$$

and

$$fSP_{Ea,3}(x_i, y_j) = y_j x_i^{ne_{3,ij}} we_{3,ij}$$

For the binary blends, the interaction parameters for the activation energy for reaction 3 are given in table 7.11.

Table 7.11: Interaction parameters for pre-exponent rate constant Ea_i in reaction 3

	i-octane/n-heptane		i-octane/methanol		n-heptane/methanol	
Reaction No.	ne	we	ne	we	ne	we
3	0.681	6470	3.00	870.00	2.30	800.00

$$f_{Ea,3}(y_{n-hept}, y_{i-oct}) = 0.53^{0.62} * 0.47^{(2-0.62)} * (5700.0) = 1428.1$$

$$fSP_{Ea,3}(x_{meth}, y_{i-oct}) = 0.47 * 0.654^{3.0} * (870.0) = 112.8$$

$$fSP_{Ea,3}(x_{meth}, y_{n-hept}) = 0.53 * 0.654^{2.3} * (800.0) = 161.1$$

$$Ea_{3,mix} = 0.47 * 10.7 \times 10^3 + 0.53 * 12.7 \times 10^3 + 1428.1 + 112.8 + 161.1 = 13.5 \times 10^3$$

To calculate$\triangle H_{rxn,3,mix}$ for reaction F3 , equation 4.40 is used.

$$\triangle H_{rxn,3,mix} = 0.47 * (20.0) + 0.53 * (20.0) = 20.0$$

When applied to all the rate constants, the complete set of rate constants are obtained below.

Table 7.12: Parameters for ternary blend used in ternary blended model F

Reaction Name	$\triangle H_{rxn}$	A	$\frac{E_a}{R}$	Pressure constant
	kJ/mol	Reaction specific	K	
F1	-284.5	2.60×10^6	18.9×10^3	-1.00
F2	2093.0	9.86×10^6	1.02×10^3	
F3	20.0	1.70×10^6	13.4×10^3	-0.5
F4+	20.0	1.67×10^{13}	22.5×10^3	-1.4
F4-	-20.0	1.43×10^{23}	37.9×10^3	
F5	4282.0	5.15×10^{15}	22.5×10^3	

Air is added to the system to obtain a stoichiometric ratio of fuel to air. This means that the initial system composition on a molar basis is 4.0% fuel, 20.1% oxygen and 75.9% nitrogen.

7.3 Heat Capacity Sample Calculation

The molar heat capacity of the system is calculated using the NASA coefficients from Thergas for the main components of the system.

Table 7.13: NASA coefficients from Thergas, valid from 1000K to 3000K

	a	b	c	d	e
carbon dioxide	4.20E+00	3.49E-03	-1.41E-06	2.55E-10	-1.71E-14
n-heptane	2.02E+01	3.52E-02	-1.11E-05	1.68E-09	-1.00E-13
nitrogen	2.80E+00	1.65E-03	-6.29E-07	1.09E-10	-7.07E-15
water	2.71E+00	3.06E-03	-9.27E-07	1.36E-10	-7.96E-15
oxygen	3.18E+00	1.60E-03	-7.09E-07	1.37E-10	-9.60E-15
methanol	3.27E+00	2.75E-03	-3.81E-07	3.17E-11	-1.30E-15
i-octane	2.33E+01	4.08E-02	-1.31E-05	2.02E-09	-1.22E-13

Table 7.14: NASA coefficients from Thergas, valid from 300K to 1000K

	a	b	c	d	e
carbon dioxide	2.26E+00	9.51E-03	-7.32E-06	2.06E-09	1.03E-14
n-heptane	-7.55E-01	8.16E-02	-4.36E-05	8.26E-09	3.84E-13
nitrogen	3.51E+00	-3.83E-04	1.25E-06	-4.37E-10	-1.37E-14
water	3.96E+00	-2.69E-04	1.94E-06	-6.13E-10	-4.49E-14
oxygen	3.08E+00	1.66E-03	-6.63E-07	1.57E-10	-4.29E-14
methanol	1.12E-01	9.61E-03	-5.04E-06	9.03E-10	8.54E-14
i-octane	3.91E+00	1.06E-01	-6.28E-05	1.15E-08	1.67E-12

At each time step the heat capacity of the system is calculated by first calculating the heat capacity of each species above using equation 4.11. For example, the heat capacity of methanol at 700K is found as follows:

$$Cp_{methanol}(700K) = 0.0112 + 9.61\times10^{-3}\times700 - 5.04\times10^{-6}\times700^2 + 9.03\times10^{-10}\times700^3 + 8.54\times10^{-14}\times700^4$$

Then the heat capacity of the fuel is calculated according to the initial molar composition of the fuel. For example, the fuel blend with 33% i-octane, 33% n-heptane and 34% methanol (by liquid volume) is converted to a molar basis, which is 16.3%, 18.3% and 65.4% for i-octane, n-heptane and methanol respectively.

$$Cp_{fuel}(700K) = 0.163 \times Cp_{i-octane}(700K) + 0.183 \times Cp_{n-heptane}(700K) + 0.654 \times Cp_{methanol}(700K)$$

The heat capacity of the final combustion product is calculated using the stoichiometric ratio of carbon dioxide to water in the blended model.

Table 7.15: Stoichiometric ratios for overall combustion of 16.3% i-octane, 18.3% n-heptane and 65.4% methanol (by moles)

Fuel		CO_2	H_2O
i-octane	C_8H_{18}	8	9
n-heptane	C_7H_{16}	7	8
methanol	CH_3OH	1	2
Ternary blend		3.24	4.24

$$Cp_{product}(700K) = \frac{4.24}{(4.24+3.24)} \times Cp_{H_2O}(700K) + \frac{3.24}{(4.24+3.24)} \times Cp_{CO_2}(700K)$$

The heat capacity of the system is then calculated based on the conversion of the fuel to product.

$$x_{conversion} = 1 - \frac{moles\ of\ fuel}{initial\ moles\ of\ fuel}$$

$$Cp_{system}(700K) = x_{N_2}Cp_{N_2}(700K) + x_{O_2}Cp_{O_2}(700K)$$

$$+(1 - x_{N_2} - x_{O_2})\left[x_{conversion}Cp_{product}(700K) + (1 - x_{conversion})Cp_{product}(700K)\right]$$

Report on Changes Made to Thesis:

Thesis Title: Development of a Generalised Kinetic Model for the Combustion of Hydrocarbon Fuels

Thesis presented for the Degree of Master of Science (Chemical Engineering) in the Department of Chemical Engineering, University of Cape Town

Author: Matthew Ryan Fry

Signature: Signed by candidate Date: 20/05/2010

Supervisor: Klaus Möller

Signature: Date: